



## RESEARCH PAPER

# Tanshinol borneol ester, a novel synthetic small molecule angiogenesis stimulator inspired by botanical formulations for angina pectoris

Sha Liao<sup>1,2</sup>  | Liwen Han<sup>3</sup> | Xiaopu Zheng<sup>4</sup> | Xin Wang<sup>5</sup> | Peng Zhang<sup>5</sup> | Jingni Wu<sup>1</sup> | Ruimin Liu<sup>1</sup> | Youlan Fu<sup>1</sup> | Jiaxin Sun<sup>1</sup> | Ximeng Kang<sup>1</sup> | Kechun Liu<sup>3</sup> | Tai-ping Fan<sup>1,2</sup> | Shao Li<sup>5</sup> | Xiaohui Zheng<sup>1</sup> 

<sup>1</sup>Key Laboratory of Resource Biology and Biotechnology in Western China, Ministry of Education, Faculty of Life Science and Medicine, Northwest University, Xi'an, China

<sup>2</sup>Angiogenesis and Chinese Medicine Laboratory, Department of Pharmacology, University of Cambridge, Cambridge, UK

<sup>3</sup>Biology Institute, Qilu University of Technology (Shandong Academy of Sciences), Jinan, China

<sup>4</sup>Department of Cardiovascular Medicine, The First Affiliated Hospital of Xi'an Jiaotong University Health Science Center, Xi'an, China

<sup>5</sup>MOE Key Laboratory of Bioinformatics and Bioinformatics Division, BNRist/Department of Automation, Tsinghua University, Beijing, China

## Correspondence

Tai-ping Fan, Department of Pharmacology, University of Cambridge, Cambridge CB2 1PD, UK.

Email: tpf1000@cam.ac.uk

Shao Li, Tsinghua University, FIT Building, Room 1-107, Beijing 100084, China.

Email: shaoli@tsinghua.edu.cn

Xiaohui Zheng, College of Life Sciences, Northwest University, No. 229 Taibai North Road, Xi'an 710069, China.

Email: zhengxh318@nwu.edu.cn

## Funding information

Opening Foundation of Key Laboratory of Resource Biology and Biotechnology in Western China (Northwest University), Ministry of Education.; Changjiang Scholars and Innovative Research Team in University, Grant/Award Number: IRT\_15R55; National Key Scientific Instrument and Equipment Development Project of China, Grant/Award Number: 2013YQ170525; National College Students Innovation and Entrepreneurship Training Project, Grant/Award Number: 201810697021; Scientific Research Plan Projects of Shaanxi Provincial Education Department, Grant/Award Number: 17JK0764; Primary R&D Plan of Shaanxi Province, Grant/Award Numbers: 2018SF-293 and 2017KW-055; National

**Background and Purpose:** Tanshinol borneol ester (DBZ) is a novel synthetic compound derived from Dantonin<sup>®</sup>, a botanical drug approved in 26 countries outside the United States for angina pectoris and currently undergoing FDA Phase III clinical trial. Here, we investigated the angiogenic effects of (S)-DBZ and (R)-DBZ isomers in vitro and in vivo.

**Experimental Approach:** A network pharmacology approach was used to predict molecular targets of DBZ. The effects of DBZ isomers on proliferation, migration, and tube formation of human endothelial cells were assessed. For in vivo approaches, the transgenic Tg (*vegfr2:GFP*) zebrafish and C57BL/6 mouse Matrigel plug models were used. ELISA and western blots were used to quantitate the release and expression of relevant target molecules and signalling pathways.

**Key Results:** DBZ produced a biphasic modulation on proliferation and migration of three types of human endothelial cells. Both DBZ isomers induced tube formation in Matrigel assay and a 12-day co-culture model in vitro. Moreover, DBZ promoted Matrigel neovascularization in mice and partially reversed the vascular disruption in zebrafish induced by PTK787. Mechanistically, DBZ enhanced the cellular levels of VEGF, VEGFR2, and MMP-9, as well as activating Akt and MAPK signalling in endothelial cells. Selective inhibition of PI3K and MEK significantly attenuated its angiogenic effects.

**Abbreviations:** CCK-8, Cell Counting Kit-8; DBZ, tanshinol borneol ester; DSS, tanshinol; HCAEC, human coronary artery endothelial cells; HCMEC, human cardiac microvascular endothelial cells; Hcy, homocysteine; HDF, human dermal fibroblasts; HIF-1, hypoxia inducible factor-1; ISVs, intersegmental vessels; MoA, mechanism of action; NBP, 3-*n*-butylphthalide; PTK787, vatalanib dihydrochloride; Raf, rapidly accelerated fibrosarcoma; Rap1, Ras-related protein 1; TCM, traditional Chinese medicine; VEGFR2, VEGF receptor 2; vWF, von Willebrand factor

Sha Liao and Liwen Han contributed equally to this work.

Natural Science Foundation of China, Grant/  
Award Numbers: 81225025 and 81630103

**Conclusions and Implications:** These data reveal, for the first time, that DBZ promotes multiple key steps of angiogenesis, at least in part through Akt and MAPK signalling pathways, and suggest it may be potentially developed further for treating myocardial infarction and other cardiovascular diseases.

## 1 | INTRODUCTION

Angiogenesis, the development of new blood vessels from pre-existing endothelium, is a dynamic multi-step process that includes extracellular matrix degradation by MMPs, endothelial cell proliferation, migration, and capillary tube formation (Hanahan & Folkman, 1996). Excessive angiogenesis leads to cancer, diabetic retinopathy, and atherosclerosis, while inadequate angiogenesis is responsible for chronic wounds, ulcers, myocardial infarcts, and possibly stroke. While many anti-angiogenic drugs (e.g., bevacizumab, sorafenib, and sunitinib) are already in clinical use, no angiogenesis stimulator, except Regranex<sup>®</sup> (becaplermin) gel for lower extremity diabetic ulcers, has entered the market mainly due to the instability of angiogenic proteins (Tirziu & Simons, 2005). As there are no other FDA-approved pro-angiogenic agents, there is an urgent need for developing small molecule angiotherapeutics for occlusive vascular disease, such as myocardial infarcts and cerebral ischaemia.

According to Newman and Cragg (2016), small molecule natural products or synthetic compounds based on natural products make up more than half of all drugs currently used in human medicine and under preclinical and clinical trial evaluation. Traditional medicinal herbs have been used for centuries for preventing and treating diseases across the globe (Zhang & Kelley, 2014) and are valuable sources for identification of lead compounds and their subsequent refinement into safe and efficacious drugs, for example, the anti-malarial artemisinin (Briggs, 2014).

Botanical formulations in traditional Chinese medicine (TCM) usually consist of several types of medicinal plants, which are thought to act in synergy to achieve a holistic therapeutic outcome (Lu et al., 2008; Wang et al., 2008). For example, composite Danshen formulations containing extracts of *Salvia miltiorrhiza* have been used in China for the treatment of cardiovascular diseases for four decades. In 1993, a new formulation Dantonic<sup>®</sup> (containing standardized extracts of *S. miltiorrhiza* and *Panax notoginseng* plus borneol) was approved by the China Food and Drug Administration as a prescription medicine for stable angina pectoris. It is currently undergoing FDA Phase III clinical trials for stable angina pectoris (ClinicalTrials.gov identifier: NCT01659580).

The pharmacologically active ingredients of a phytocomplex such as TCM compound formulations (*fufang*) are not always the original natural molecules but may be their host-specific metabolites or molecular complexes formed following co-administration of selected herbs. We have previously discovered an active Dantonic metabolite (isopropyl 3-(3,4-dihydroxyphenyl)-2-hydroxy-propanoate, IDHP) and found it was a NO-independent vasodilator, which attenuated cardiac fibrosis in rats as well (Zheng, Zhao, Zhao, et al., 2007; Yin et al.,

### What is already known

- DBZ is a novel synthetic compound derived from a botanical drug for angina pectoris.

### What this study adds

- DBZ promoted multiple key steps of angiogenesis through Akt and MAPK signalling pathways.

### What is the clinical significance

- DBZ may be potentially developed further for treating myocardial infarction and other cardiovascular diseases.

2015). Tanshinol (DSS, (+)  $\beta$ -(3,4-dihydroxyphenyl) lactic acid) is the primary ingredient in an aqueous extract of *S. miltiorrhiza* and exhibits pleiotropic activities, such as protection of vascular endothelial cells against homocysteine (Hcy)-induced damage (Chan et al., 2004) and protection of myocardium from ischaemia/reperfusion injury (Yang et al., 2015). However, as a hydrophilic molecule, DSS is poorly soluble in lipidic matrices and difficult to enter cells by crossing the cell membrane (Dong, Wang, & Zhu, 2009). According to the principle of TCM combinatorial formulations (Qiu, 2007; Zhao et al., 2015), borneol is believed to improve the bioavailability of principal therapeutic agents (Cai et al., 2008; Chen et al., 1990; Yang et al., 2009). In our previous studies in rabbits, the bioavailability of DSS was found to increase, and the tissue distribution was improved by co-administration of borneol (Zheng, Zhao, Fang, et al., 2007; Liu et al., 2008).

Inspired by these findings, we developed a drug design strategy (Combination of Traditional Chinese Medicine Molecular Chemistry; Zheng, Jia, & Bai, 2015). Using this strategy, biologically active lead structures or fragments, stemming from different herbs in the “composite formulae” (*fufang*), were selected or optimized without losing their functionalities and then constructed into a set of brand new molecules by chemosynthetic means in the light of compatibility principle of TCM (Qiu, 2007; Zhao et al., 2015). In a previous study, we designed and synthesized tanshinol borneol ester (DBZ, 1,7,7-trimethylbicyclo[2.2.1]heptan-2-yl-3-(3,4-dihydroxyphenyl)-2-hydroxy-propanoate) by chemical combination of tanshinol (DSS) and borneol (core effective components of Dantonic) as well as a library of related compounds according to our drug design strategy. Here, we used a network pharmacological approaches (Li & Zhang, 2013) to predict the molecular targets of DBZ, validated its pro-angiogenic activities in vitro and in vivo, of its two isomers, and elucidated their mechanisms of action.

## 2 | METHODS

### 2.1 | Target prediction and functional enrichment analysis

In silico prediction of potential targets of DSS, borneol, and DBZ was conducted by drugCIPHER (Zhao & Li, 2010), a state-of-art network-based algorithm for global prediction of drug–target interactions. In principle, this algorithm predicts relationships between compounds and targets through network-based integration of multiple pharmacological similarities among drugs and network interactions among targets. In order to obtain high-confidence results, the top 100 predicted targets of each compound were selected for the following mechanism of action (MoA) analysis. To identify the MoA of DSS, borneol, and DBZ, we investigated the enrichment of the high-confidence targets of these three compounds and network neighbour bioactive molecules in literatures of DSS and borneol in the Kyoto Encyclopedia of Genes and Genomes pathways through the Fisher exact test (Huang, Sherman, & Lempicki, 2009). We selected significantly enriched pathways with  $P < .05$  after Benjamin's correction, as described in Table S1.

### 2.2 | Network construction

Previous studies indicated that for a drug considered as a multi-target therapy, a network approach is adopted to represent and analyse the complex biological system underlying the drug's actions (Barabási, Gulbahce, & Loscalzo, 2011). Based on the high-confidence targets of DBZ and key proteins in significantly enriched pathways of DBZ, we constructed a network targeted by DBZ to identify its MoA based on the protein–protein interactions.

### 2.3 | Cells and culture conditions

Heterogeneity of the endothelium not only occurs in different organs but also between the macro- and microvasculature, and these differences may be reflected in the phenotype of cultured endothelial cells (Staton, Lewis, & Bicknell, 2007). In the present work, HUVEC, human coronary artery endothelial cells (HCAEC), and human cardiac microvascular endothelial cells (HCMEC) were employed to investigate the angiogenic effect of DBZ in vitro. HUVEC, HCAEC, HCMEC, and normal human dermal fibroblasts (HDF) were all purchased from PromoCell (Heidelberg, Germany). HUVEC (Cat# 12203) were maintained in Endothelial Basal Medium supplemented with Endothelial Cell Growth Medium SupplementPack (PromoCell), while HCAEC (Cat# 12221), and HCMEC (Cat# 12285) were maintained in Endothelial Basal Medium MV supplemented with Endothelial Cell Growth Medium MV SupplementPack (PromoCell). HDF (Cat# 12300) were maintained in DMEM with 10% FBS (Life Science, Paisley, UK). All cells were grown at 37°C under a humidified atmosphere with 5% CO<sub>2</sub>.

### 2.4 | Cell proliferation assay

Cells were seeded in complete medium (basal media containing FBS and growth supplements) in 96-well plates for Cell Counting Kit-8 (CCK-8) assays and seeded in six-well plates for trypan blue exclusion assays, respectively. The next day, complete medium was removed and renewed with growth supplement-free low serum (0.5% FBS) medium. After starvation, the medium was replaced with supplement-free medium with different concentrations of (S)-DBZ and (R)-DBZ, respectively. After a 48-hr incubation, cell viability was measured by CCK-8 (Dojindo, Kumamoto, Japan) according to the manufacturer's instructions. In another set of experiments, HUVEC were pretreated with DBZ for 2 hr and then challenged with 5-mM homocysteine (Hcy). After 48-hr incubation, total cells were collected by a brief trypsinization, and viable cells were counted by trypan blue exclusion using Countess II FL Automated Cell Counter (Invitrogen, Carlsbad, USA).

### 2.5 | Endothelial wound healing assay

Cells were seeded in 24-well plates containing a Thermanox™ plastic coverslip (Thermo Fisher Scientific, Waltham, USA) in each well pre-coated with 1.5% gelatin. On reaching confluence, the cover slips were collected and the cells were wounded using a multi-channel wounder designed by ourselves (Lauder, Frost, Hiley, & Fan, 1998). The wounded monolayer was rinsed and then incubated with basal medium containing 0.5% FBS with various concentrations of test compounds for 8 hr. Images of the wounds were recorded (40×) with an inverted microscope (Leica DMI 3000B, Wetzlar, Germany). The distance between the wound margins and cell number was measured by ImageJ software v1.60 (NIH, Bethesda, USA).

### 2.6 | Transwell migration assay of endothelial cells

The migration ability of HUVEC was tested in the Transwell Boyden Chambers (6.5 mm; Costar Corporation, Cambridge, USA). The polycarbonate membranes (8-µm pore size) on the bottom of the upper compartment of the transwells were coated with 0.1% gelatin matrix. Medium containing vehicle or test compounds was placed in the bottom wells of the chamber. The upper chamber was loaded with  $3 \times 10^4$  cells, and the transwell-containing plates were incubated for 4 hr. At the end of the incubation, cells that had migrated to the lower surface of the filter membrane were fixed with 90% ethanol and stained with 0.1% crystal violet. Images of migrant cells were captured by a photomicroscope (Leica DMI 3000B). Cell migration was quantified by blind counting of the migrated cells on the lower surface of the membrane using ImageJ software v1.60 (NIH), with five fields per chamber.

### 2.7 | In vitro Matrigel tube formation assay on HUVEC

HUVEC were plated into 96-well plates coated with growth factor-reduced Matrigel (BD, Oxford, UK) and incubated for 6 hr at 37°C in

growth supplement-free medium in the presence of test compounds as indicated. All images were visualized using a photomicroscope (Leica DMI 3000B). To quantify tube formation, junctures at which at least three tubes converged were counted in each well in a blinded manner.

## 2.8 | Co-culture tube formation assay

In the 12-day co-culture model, when human fibroblasts are co-cultured with endothelial cells, the fibroblasts secrete the necessary matrix components that act as a scaffold for tube formation (Bishop et al., 1999). In contrast to the 6-hr Matrigel assay, this 12-day assay has been shown to produce tubes that contain lumen, and a more heterogeneous pattern of tube lengths that more closely resemble capillary beds in vivo (Bishop et al., 1999). Briefly, HDF were switched over to endothelial complete medium a day before seeding. Cells were then seeded at a ratio of 1:20 (HUVEC : NHDF) in endothelial complete medium in 96-well plates. After 2 days, the medium was replenished, and then on Day 4, medium was changed to low growth supplement (10%) medium and the drug added. Human recombinant **VEGF-A** (20 ng·ml<sup>-1</sup>; Invitrogen, Paisley, UK) was used as a positive control. We changed the media and added the test compounds every 2 days. At Day 12, cells were fixed with 10% formalin, incubated with an rabbit anti-human-**von Willebrand factor** (vWF) monoclonal IgG (1:1,000; Sigma-Aldrich, Gillingham, UK; Cat# F3520, RRID: AB\_259543; Bishop et al., 1999), and then a mouse anti-rabbit alkaline phosphatase conjugated IgG (1:1,000; Sigma-Aldrich; Cat# A9919). Following washes, one-Step™ NBT/BCIP kit (ThermoScientific, Loughborough, UK) was applied until a suitable signal was developed. Images of two fields of view were taken per well. The total tube area and average tube size of vWF-positive endothelial cells forming capillary-like tubes were quantified by the ImageJ software v1.60 (NIH).

## 2.9 | ELISA

Cells were seeded in 96-well plates at a density of  $1.5 \times 10^4$  cells·ml<sup>-1</sup>. When they had reached 70–80% confluence, cells were incubated with test compounds in serum-free, growth factor-free medium for the indicated times, and medium was collected and analysed for secreted VEGF level by using a commercially available ELISA kit (R&D Systems, Minneapolis, USA) according to the manufacturer's instructions. Absorbance was measured at 450 nm using a microplate reader (PerkinElmer, Waltham, USA).

## 2.10 | Western blot analysis

The immuno-related procedures used comply with the recommendations made by the *British Journal of Pharmacology*. HUVEC were treated with 10 nmol·L<sup>-1</sup> (S)-DBZ or (R)-DBZ for different time durations in the time course study. To observe dose-dependent effects of DBZ, cells were treated with different concentrations of (S)-DBZ or (R)-DBZ for 60 min or for 24 hr as indicated. For inhibition assays, cells were pretreated with **LY294002** or **U0126** respectively for

30 min prior to the addition of DBZ (10 nM). Then cells were rinsed with ice-cold PBS and lysed in ice-cold RIPA buffer (50-mM TrisCl, pH 7.4, 150-mM NaCl, 0.1% SDS, 1% sodium deoxycholate, and 1% Triton-X 100) with the addition of protease and phosphatase inhibitor cocktail (Abcam, Cambridge, UK; Cat# ab201120). Cell extracts were centrifuged for 20 min at 4°C and evaluated for protein concentration. Afterwards, samples were denatured for 5 min at 95°C and subjected to 10% SDS-PAGE. After electrotransfer on 0.45-µm PVDF membranes (GE Healthcare, Buckinghamshire, UK), proteins were blocked in TBST (Tris-buffered saline with 0.1% Tween-20) with 5% protease free BSA (Sigma-Aldrich, Cat# B2064) or nonfat dry milk (for β-actin) and then subjected to a 4°C overnight incubation with the indicated antibodies followed by 1-hr incubation at room temperature with HRP-coupled secondary antibodies. Immunoreactive bands of proteins were detected with ECL-Plus chemiluminescence reagents (GE Healthcare, Little Chalfont, UK). The Spectra™ Multicolor Broad Range protein ladder (ThermoScientific; Cat# 26634) was included on all gels. All the antibodies were diluted in TBST with 5% BSA or nonfat dry milk (for β-actin and secondary antibodies), maintained at 4°C and re-used up to twice within 4 days. The following antibodies were used: rabbit anti-**Akt** monoclonal IgG (1:1,000; Cell Signalling Technology, Hitchin, UK; Cat# 4691, RRID:AB\_915783), rabbit anti-p-Akt monoclonal IgG (1:2,000; Cell Signalling Technology; Cat# 4060), rabbit anti-**PLCγ** monoclonal IgG (1:1,000; Cell Signalling Technology; Cat# 5690, RRID:AB\_10695542), rabbit anti-p-PLCγ polyclonal IgG (1:1,000; Cell Signalling Technology; Cat# 2821, RRID:AB\_330855), rabbit anti-**Raf-1** polyclonal IgG (1:1,000; Cell Signalling Technology; Cat# 9422, RRID:AB\_390808), rabbit anti-p-Raf-1 polyclonal IgG (1:1,000; Cell Signalling Technology; Cat# 9421, RRID:AB\_330759), rabbit anti-**ERK1/2** monoclonal IgG (1:1,000; Cell Signalling Technology; Cat# 4695, RRID:AB\_390779), rabbit anti-p-ERK1/2 monoclonal IgG (1:2,000; Cell Signalling Technology; Cat# 4370, RRID: AB\_2315112), rabbit anti-**MMP-9** polyclonal IgG (1:1,000; Cell Signalling Technology; Cat# 2270, RRID:AB\_2144612), rabbit anti-**VEGFR2** monoclonal IgG (1:1,000; Cell Signalling Technology; Cat# 9698, RRID:AB\_11178792), mouse anti-β-actin monoclonal IgG2b (1:1,000; Cell Signalling Technology; Cat# 3700, RRID:AB\_2242334), HRP-linked goat anti-rabbit IgG (1:1,500; Cell Signalling Technology; Cat# 7074, RRID:AB\_2099233), and HRP-linked horse anti-mouse IgG (1:2,000; Cell Signalling Technology; Cat# 7076, RRID:AB\_330924). The density of each immunoblot band was scanned by ImageJ software v1.60 (NIH), and the ratios of phosphorylated protein/total protein or target protein/β-actin protein were calculated in the corresponding samples from the same blot, respectively, which was used as a loading control to minimize variances. Data were collected and analysed from five independent samples, and the investigators were blinded to the treatment.

## 2.11 | Animal welfare and ethical statements

Animal studies are reported in compliance with the ARRIVE guidelines and with the recommendations made by the *British Journal of*



*Pharmacology* (Kilkenny et al., 2010). Zebrafish experiments were approved by the Animal Ethics Committee in the Biology Institute of Shandong Academy of Sciences (approval no. BISD-20180011), and murine Matrigel experiments were approved by the Northwest University Ethics Committee on Animal Research and Welfare (approval no. NWU-AWC-20190102M). All the animal care and experimental procedures were carried out in accordance with the regulations of experimental animal administration issued by the State Committee of Science and Technology of People's Republic of China on November 14, 1988, and the National Institutes of Health Guide for the Care and Use of Laboratory Animals (8th Edition, Institute for Laboratory Animal Research). In particular, humane endpoints were implemented in this study involving animals based on the National Guideline for Replacement, Refinement and Reduction of Animals in Research in China (GB/T 27416-2014). Efforts were made to minimize animal suffering. Animals were anaesthetized when it was likely they could be subjected to pain, and they were killed by a method that ensured the least effect on their welfare.

## 2.12 | Animals

Transgenic zebrafish (Tg [*vegfr2:GFP*]) that express GFP in the developing vasculature were obtained from the Biology Institute of Shandong Academy of Sciences (donated by Prof. Jingwei Xiong, Institute of Molecular Medicine, Peking University) and were maintained in 3-L polystyrene aquarium tanks (15 zebrafish per tank) with constant aeration and flow water systems at 28.5°C under a 14-hr light/10-hr dark photoperiod. Food with brine shrimp was fed twice per day. For breeding, adult zebrafish were placed in 1.5-L breeding tanks overnight and were separated by a transparent barrier that was removed on the following morning.

Male C57BL/6 mice (7–8 weeks of age,  $22 \pm 2$  g) were purchased from the Experimental Animal Centre in Xi'an Jiaotong University (Shaanxi, China). The mice were acclimatized for 1 week after arrival and maintained under specific pathogen-free conditions. Animals were housed in polycarbonate cages of 18 cm × 35 cm (two mice per cage) with standard sawdust as bedding and maintained under controlled conditions of temperature at 22–24°C, humidity at  $60 \pm 5\%$ , and alternating light/dark cycles (lights were on between 7:00 hr and 19:00 hr) and fed with standard laboratory chow and water ad libitum. Caging equipment was sterilized, and the food irradiated, and water filtered. A total of 48 mice were used in the experiments described here.

## 2.13 | In vivo zebrafish assays

Zebrafish embryos were generated by natural pair-wise mating (12–14 months old) and raised in culture water (containing 5.00-mM NaCl, 0.17-mM KCl, 0.44-mM CaCl<sub>2</sub>, 0.16-mM MgSO<sub>4</sub>). Healthy, hatched zebrafish embryos were picked out and staged by time and morphological criteria (Cannon, Upton, Smith, & Morrell, 2010). Randomization was used to assign embryos to different experimental

groups and to the drug treatment. Experiments were performed in 24-well microplates with 10 embryos per well. PTK787 (vatalanib dihydrochloride, MedChem Express, Monmouth Junction, USA), 3-*n*-butylphthalide (NBP, positive control), (S)-DBZ, (R)-DBZ, DSS, and borneol were dissolved in DMSO and then further diluted in culture water to the required concentrations; 24 hr post-fertilization (hpf) embryos in culture water were treated with test compounds for 24 hr at 28.5°C with a 14-hr light/10-hr dark cycle. Control embryos were treated with the equivalent amount of DMSO solution (final concentration: 0.1% DMSO [v/v]). To characterize the intersegmental vessels (ISVs), embryos were dechorionated with 1 mg·ml<sup>-1</sup> of Pronase E (Solarbio, Shanghai, China) before treatment. Embryos were anaesthetized with 0.02% tricaine methanesulfonate and photographed under a fluorescence microscope (Olympus SZX16, Tokyo, Japan). The length of ISVs between the trunk and tail of each embryo was measured with the ImageJ software v1.60 (NIH) by a user blinded to the exposure groups. A total of 90 embryos were evaluated for each experimental condition, and each experiment was repeated five times. No adverse event was observed in each experimental group.

## 2.14 | In vivo Matrigel plugs assays

We used the C57BL/6 mouse Matrigel plug model of angiogenesis introduced by Zudaire and Cuttitta (2012) and Murray (2001). This widely used model is particularly useful for studying neovascularization as it provides a more natural environment for endothelial cell recruitment and capillary formation (Zudaire & Cuttitta, 2012) and provides the opportunity for quantifying the effect of angiogenic stimulators and inhibitors more easily than others (CAM and rabbit corneal assay; Jain, Schlenger, Hockel, & Yuan, 1997). The drug can either be placed in the plug together with the test factor by mixing with the Matrigel matrix or be given to the host animal (Nowak-Sliwinska et al., 2018). To investigate whether systemic administration of DBZ exhibits pro-angiogenic effect, 48 mice were randomly assigned into six groups (eight mice per group), and the group size was based on the consensus guidelines for the use and interpretation of angiogenesis assays (Nowak-Sliwinska et al., 2018), our previous studies, and power calculations (The power analysis was performed using G\*power software suggests at least  $n = 5$  are needed [ $\alpha = .05$ , power  $(1-\beta) = 0.90$ , effect size = 0.892]). An aliquot (500 µl) of phenol red free GFR-Matrigel (BD, Bedford, USA) was injected s.c. into both groin areas of mice after anaesthesia with 1.25% avertin (0.2 ml·10 g<sup>-1</sup>, i.p. injection) and monitored by surveillance of reflex absence. Matrigel plugs premixed with bFGF (150 ng·ml<sup>-1</sup>; PeproTech, Rocky Hill, USA) and heparin (64 u·ml<sup>-1</sup>) served as a positive control. Then mice were administered either vehicle (0.2% poloxamer 188 [BASF, Ludwigshafen, Germany] solution for control and positive control groups) or different doses of DBZ (0.2, 1, 5, and 25 mg·kg<sup>-1</sup> in the vehicle) once a day (10:00 am) by i.p. injections for eight consecutive days, respectively. For each group, a cage was randomly selected from the pool of all cages. The randomized treatment administrations were

performed to simultaneously assess the effect of different treatments and avoid time-variable environmental influences. The doses of DBZ used in the experiments were based on a pilot study and the Good Laboratory Practice toxicology studies in mice by i.v. injection ( $LD_{50} = 460.700 \pm 26.107 \text{ mg}\cdot\text{kg}^{-1}$ ) by National Beijing Center for Drug Safety Evaluation and Research. After 8 days, mice were killed in a  $\text{CO}_2$  chamber. All efforts were made to minimize the number of animals used and their suffering. No adverse event was observed in each experimental group. The Matrigel plugs from both groin areas were removed, weighed, and homogenized (one plug per mouse) in 1-ml deionized  $\text{H}_2\text{O}$  on ice and cleared by centrifugation at  $10,100\times g$  for 5 min at  $4^\circ\text{C}$ . The supernatant was collected, and the haemoglobin content was determined using the Drabkin reagent kit according to the manufacturer's protocol (Sigma-Aldrich, St Louis, USA). The absorbance was measured in a microplate reader (PerkinElmer, Waltham, USA) at 540 nm and normalized to the plug weight.

To further investigate the potential angiogenic effect of DBZ *in vivo*, haematoxylin and eosin (H&E) staining and immunofluorescence staining were performed. Briefly, the Matrigel plugs (one plug per mouse) were fixed in 4% paraformaldehyde solution, processed, embedded, sectioned, and either H&E stained, or blocked (TBS with 10% donkey serum, 1% BSA, 0.3-M glycine, and 0.3% Triton-X 100) and incubated with primary antibody: rabbit polyclonal anti-CD31 IgG (1:150; Abcam, Cambridge, UK; Cat# ab28364, RRID: AB\_726362). Negative controls were incubated without primary antibodies. Sections were then stained with donkey anti-rabbit IgG H&L secondary antibody Alexa Fluor 488 (1:800; Abcam; Cat# ab150073, RRID:AB\_2636877) and counterstained with DAPI ( $5 \mu\text{g}\cdot\text{ml}^{-1}$ ; Roche, Mannheim, Germany; Cat# 10236276001). All the antibodies were diluted in TBS containing 1% BSA and not re-used. The H&E images were obtained on an Invitrogen EVOS M5000 microscopy, and immunofluorescence images were obtained by a laser-scanning confocal microscope (FV1000, Olympus, Japan) equipped with FV10-ASW 4.0 VIEW (Olympus), and the investigators were blinded to the treatment. The immunoreactive areas were quantified using ImageJ software v1.60 (NIH), and the histological analyses and the data analyses were blinded to the treatment.

## 2.15 | Data and statistical analysis

The data and statistical analysis comply with the recommendations of the *British Journal of Pharmacology* on experimental design and analysis in pharmacology (Curtis et al., 2018). Data are presented as mean  $\pm$  SD for  $n \geq 5$ . In each experiment,  $n$  represents the number of independent experiments (in vitro and zebrafish assays) and the number of mice per group (in vivo Matrigel plug assays). Technical replicates were only used to ensure the reliability of single values. The  $n$  value included for statistical tests is shown in the figure legend. This is adopted based on our previous results (Leung et al., 2007; Sengupta et al., 2004) and power analysis (G\*power 3.1.9.3 software; RRID: SCR\_013726) and also for the purpose of carrying out statistical

analysis according to the guidelines of *BJP* (Curtis et al., 2018). All subjects were randomly assigned into groups resulting in equal sample sizes by an online randomizer (GraphPad QuickCalcs: <https://www.graphpad.com/quickcalcs/randomize1.cfm>), and all treatments were randomized to avoid systematic bias. All the quantifications and data analysis were blinded; thus, the analyst did not know the origin of the data during quantification of samples and statistical analysis. No data points were excluded from the analysis in any experiment. Data normalization was undertaken to control for sources of variation of baseline parameters and to allow comparison of the magnitude of drug effects in different conditions. All analyses were performed using GraphPad Prism 7.0 software (GraphPad Software, La Jolla, CA, USA). The normality of the data distribution was tested by the Shapiro–Wilk test and Kolmogorov–Smirnov normality test. Statistical significance was determined using Student's unpaired two-tailed  $t$  test or unpaired  $t$  test with Welch's correction when comparing two groups, and one-way ANOVA followed by Dunnett's post hoc test (only if  $F$  was significant, and there was no significant variance inhomogeneity) or Kruskal–Wallis test with Dunn's post hoc test when comparing multiple groups. A  $P$  value of less than .05 was considered significant.

## 2.16 | Materials

(S)-DBZ and (R)-DBZ (United States patent no. 8017786) were synthesized by us, using the method described by Bai et al. (2014). Other chemicals were all obtained from Sigma-Aldrich unless otherwise specified.

## 2.17 | Nomenclature of targets and ligands

Key protein targets and ligands in this article are hyperlinked to corresponding entries in <http://www.guidetopharmacology.org>, the common portal for data from the IUPHAR/BPS Guide to PHARMACOLOGY (Harding et al., 2018), and are permanently archived in the Concise Guide to PHARMACOLOGY 2017/18 (Alexander et al., 2017a, 2017b).

## 3 | RESULTS

### 3.1 | In silico prediction and network analysis of potential targets and function of DBZ

Comprehensive targets are used to determine the biological activities of herbal compounds by mapping them on signalling pathways (Besnard et al., 2012). In this study, a computational workflow based on network pharmacology methods was applied to predict potential targets and characterize their mechanism of combinational actions of DBZ. It is regarded as a representative method of emerging network pharmacology (Barabási et al., 2011) and has been successfully applied in analysis of the MoA for TCM (Liang, Li, & Li, 2014). Potential regulated pathways based on potential target of DBZ, DSS, and borneol

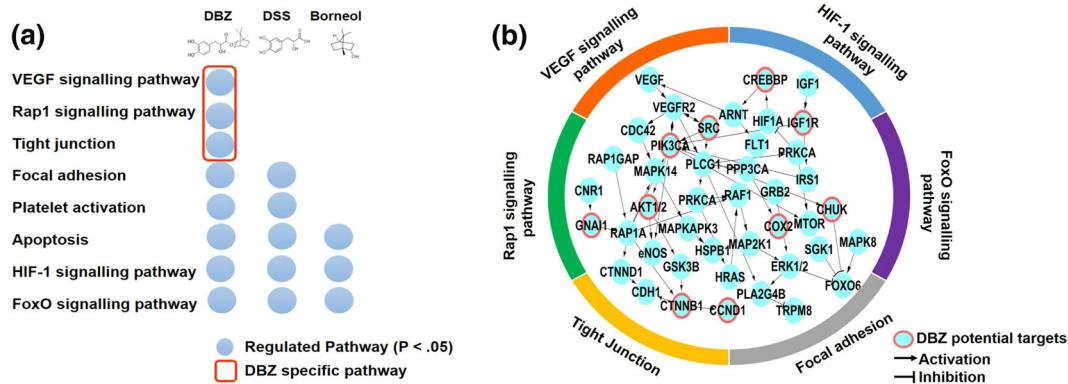


**FIGURE 1** In silico prediction and network analysis of potential targets and function of DBZ. (a) Comparison of enriched Kyoto Encyclopedia of Genes and Genomes pathways of DBZ, DSS, and borneol ( $P < .05$ ). (b) Functional subnetwork perturbed by DBZ. Red circles are directly predicted targets, and other nodes are in the enriched pathway of DBZ

are described in Figure 1a and Table S1. Except common pathways such as “HIF-1 signalling pathway,” “FoxO signalling pathway,” “Apoptosis,” and “Focal adhesion,” DBZ has its specific pathways including “VEGF signalling pathway,” “Rap1 (Ras-related protein 1) signalling pathway,” and “Tight junction.”

The genes or proteins involved in these pathways were mapped in the protein–protein interaction network. As shown in Figure 1b, the DBZ potential targets as “seed nodes” to connected subnetwork. PIK3CA, AKT1/2, CREBBP, IGF1R, and SRC (rank top 5% in the target list) as key genes are highly connected nodes within the regulatory network of DBZ. Our work demonstrated that potential targets of DBZ could regulate the VEGF signalling pathway related biological process to mediate the angiogenic activities of DBZ (Figures 1b and 7g). Therefore, we examined the potential effects of DBZ on angiogenesis in vitro and in vivo.

### 3.2 | Effects of (S)-DBZ and (R)-DBZ on endothelial cell proliferation and motility

As determined by the CCK-8 assay, (R)-DBZ stimulated proliferation on HUVEC, HCMEC, and HCAEC after 48-hr treatment, whereas (S)-DBZ exerted no promoting effect (Figure S1). However, both (S)-DBZ and (R)-DBZ inhibited HUVEC proliferation at the highest concentration (1,000 nM; Figure S1C); thus, we choose 100 nM as the maximum concentration in further studies. In trypan blue assays, both (S)-DBZ and (R)-DBZ showed significant protective effect on HUVEC viability against Hcy-induced injury (Figure S2A–D).

Next, we studied the effects of DBZ on the migratory and invasive properties of endothelial cells using wound healing and Transwell assays, respectively. In wound healing assays, the distance between the wound margins of HUVEC and the number of migrated HCMEC were determined. As shown in Figure 2a,b, both (S)-DBZ and (R)-DBZ treatment for 8 hr significantly increased the wound closure on HUVEC compared to the control. Besides, both (S)-DBZ and (R)-DBZ caused significantly higher number of HCMEC migrating into the wounds compared to the control (Figure 2c,d). In transwell chamber

assays, both (S)-DBZ and (R)-DBZ significantly induced migration of HUVEC from the upper chamber to the lower chamber (Figure 2e,f), which was a biphasic modulation, and the effect was greatest when (S)-DBZ and (R)-DBZ was at 1 nM, respectively. Above all, both (S)-DBZ and (R)-DBZ could increase motility in human endothelial cells.

### 3.3 | Induction of capillary-like tube formation by (S)-DBZ and (R)-DBZ in HUVEC

To explore the effect of DBZ on the formation of tubular structures by endothelial cells, we first used the in vitro Matrigel-based assay. A very low level of tube formation was observed when HUVEC were seeded on growth factor-reduced Matrigel in low serum medium for 6 hr, whereas morphological changes were observed after treatment with (S)-DBZ (Figure 3a). Quantitative analysis indicates that (S)-DBZ significantly stimulated HUVEC to form more branching points compared to the control group, reaching a maximum at 10 nM. Similarly, (R)-DBZ-induced HUVEC to form more extensive capillary-like networks on Matrigel compared to control group (Figure 3b).

### 3.4 | Effects of (S)-DBZ, (R)-DBZ, DSS, and borneol on tube formation in a co-culture model

In a 12-day HUVEC and fibroblasts co-culture model, the endothelial cells rely on the fibroblasts to form tubes, and the growth factor profile is much more characterizable than that of Matrigel. As shown in Figure 3c,d, both (S)-DBZ and (R)-DBZ treatment significantly enhanced capillary-like tube formation in the co-culture model compared to vehicle control and up to a peak at 1 nM, respectively. Those observational findings were confirmed by the quantitative results of the total tube area and average tube size. A significant increase in tube formation was also observed in VEGF-treated cells which served as a positive control. In contrast, DSS showed less potent effect on tube formation compared to (S)-DBZ and (R)-DBZ,



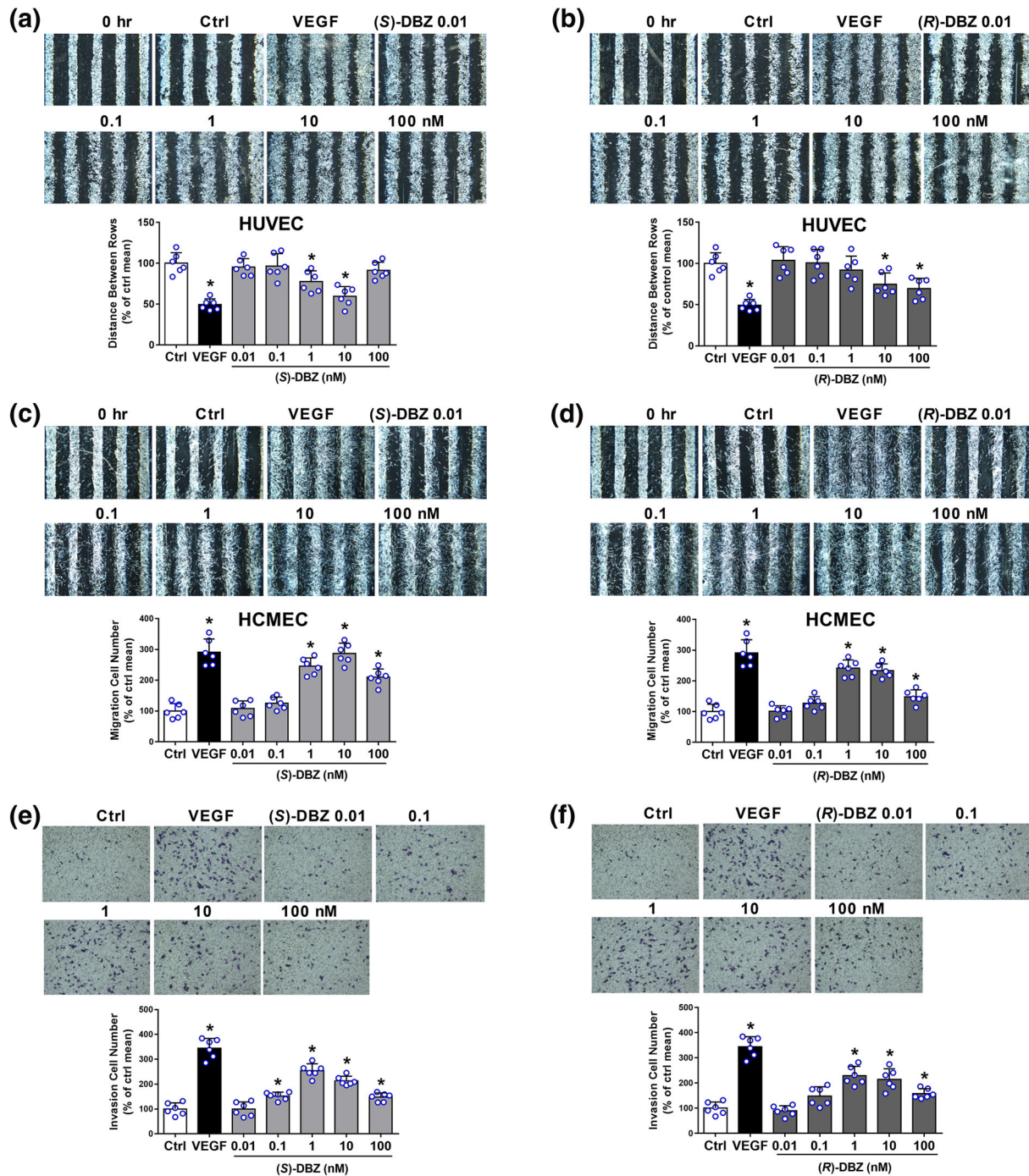


**FIGURE 2** (S)-DBZ and (R)-DBZ promoted the motility of endothelial cells. Effects of (S)-DBZ (a, c) and (R)-DBZ (b, d) on the migratory potential of HUVEC and HCMEC were investigated by wound healing assay. Representative photomicrographs are shown at 40× magnification, and wound healing was evaluated by measuring the distance between the wound margins (HUVEC) or by counting cell numbers (HCMEC). Effects of (S)-DBZ (E) and (R)-DBZ (F) on the invasive potential of HUVEC were examined using transwell invasion chambers. Representative photomicrographs showing the stained cells on the lower side of membranes. Human recombinant VEGF-A ( $20 \text{ ng}\cdot\text{ml}^{-1}$ ) was used as a positive control. Results are expressed as the mean percentage of control mean (means  $\pm$  SD,  $n = 6$  independent experiments performed in duplicate for wound healing assays,  $n = 6$  independent experiments performed in triplicate for transwell migration assays). \* $P < .05$  compared with Ctrl group. Statistical analyses were performed by one-way ANOVA followed by Dunnett's post hoc test or Student's unpaired two-tailed  $t$  test. HCMEC, human coronary artery endothelial cells

and borneol had no effect on tube formation at all (Figure 3e). All these data indicated that chemical linkage of DSS and borneol to form DBZ greatly enhanced the pro-angiogenic activity of parent

compounds. Furthermore, both (S)-DBZ and (R)-DBZ significantly protected HUVEC against Hcy-induced vascular disruption in co-culture models (Figure S2E,F).



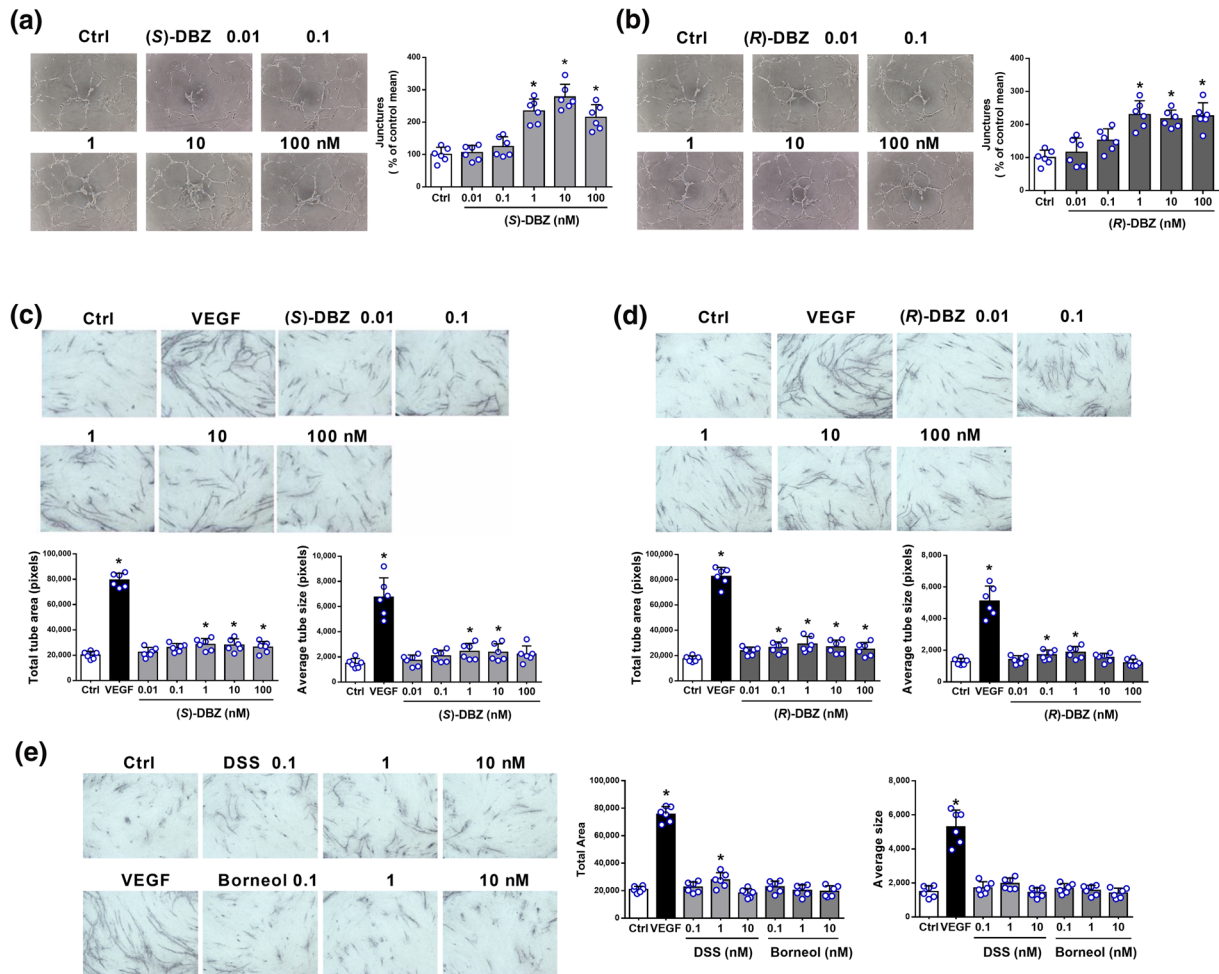


**FIGURE 3** Induction of tube formation by (S)-DBZ and (R)-DBZ in Matrigel and HUVEC-HDF co-culture models. Effects of (a) (S)-DBZ and (b) (R)-DBZ on the capillary tube formation of HUVEC were examined by plating HUVEC on the Matrigel. After 6 hr, tubular structures were photographed, and the number of tube junctions was counted. Co-cultures of human endothelial cells and dermal fibroblasts were treated with (c) (S)-DBZ, (d) (R)-DBZ, (e) DSS, and borneol. Human VEGF-A ( $20 \text{ ng}\cdot\text{ml}^{-1}$ ) was used as a positive control. On Day 12, the co-cultures were fixed and stained for vWF, and then total tube area and average tube size was quantified by the ImageJ software. Magnification: 40 $\times$ . Results are expressed as means  $\pm$  SD ( $n = 6$  independent experiments performed in triplicate for Matrigel assays;  $n = 6$  independent experiments with five wells each for co-culture assays). \* $P < .05$  compared with Ctrl group. Statistical analyses were performed by one-way ANOVA followed by Dunnett's post hoc test or Student's unpaired  $t$  test, or unpaired  $t$  test with Welch's correction. DSS, tanshinol

### 3.5 | Effects of (S)-DBZ and (R)-DBZ on VEGF secretion, VEGFR2, and MMP-9 protein expression in HUVEC

Because VEGF is known to be a key activator of angiogenesis, we examined whether this growth factor is up-regulated by DBZ. As determined by ELISA, treatment with (S)-DBZ or (R)-DBZ for 48 hr increased the level of VEGF protein secretion in the culture medium, with (R)-DBZ being more potent than (S)-DBZ (Figure 4a,b). As shown in Figure 4c,d, the expression of VEGFR2 was significantly increased after incubation with different concentrations of (S)-DBZ and (R)-DBZ, reaching the maximum at a concentration of 100 nM and 1 nM, respectively. In addition, both (S)-DBZ and (R)-DBZ significantly promoted the MMP-9 expression compared to the control (Figure 4e,f). Hence, these results suggest that the up-regulation of expression of these proteins caused by DBZ could contribute to its pro-angiogenic effects.

### 3.6 | (S)-DBZ and (R)-DBZ activated Akt and MAPK pathways

Akt (also known as PKB) and ERK1/2, one of the major targets of the MAPK signalling pathway, have been implicated in the regulation of angiogenesis for different functions including cell proliferation, migration, and survival (Hoeben et al., 2004). As shown in Figure 5a,b, both (S)-DBZ and (R)-DBZ stimulated the phosphorylation of Akt in a time-dependent manner. The ratios of p-Akt/Akt were significantly enhanced after treatment with DBZ as well. (S)-DBZ (10 nM) treatment significantly increased the phosphorylation from 30 min and reached a maximum level at 120 min, whereas the phosphorylation being detected at 60 min in (R)-DBZ (10 nM) treated cells. Furthermore, phosphorylation of Akt in HUVEC was enhanced after incubation with different concentrations of (S)-DBZ (Figure 5c) or (R)-DBZ (Figure 5d).

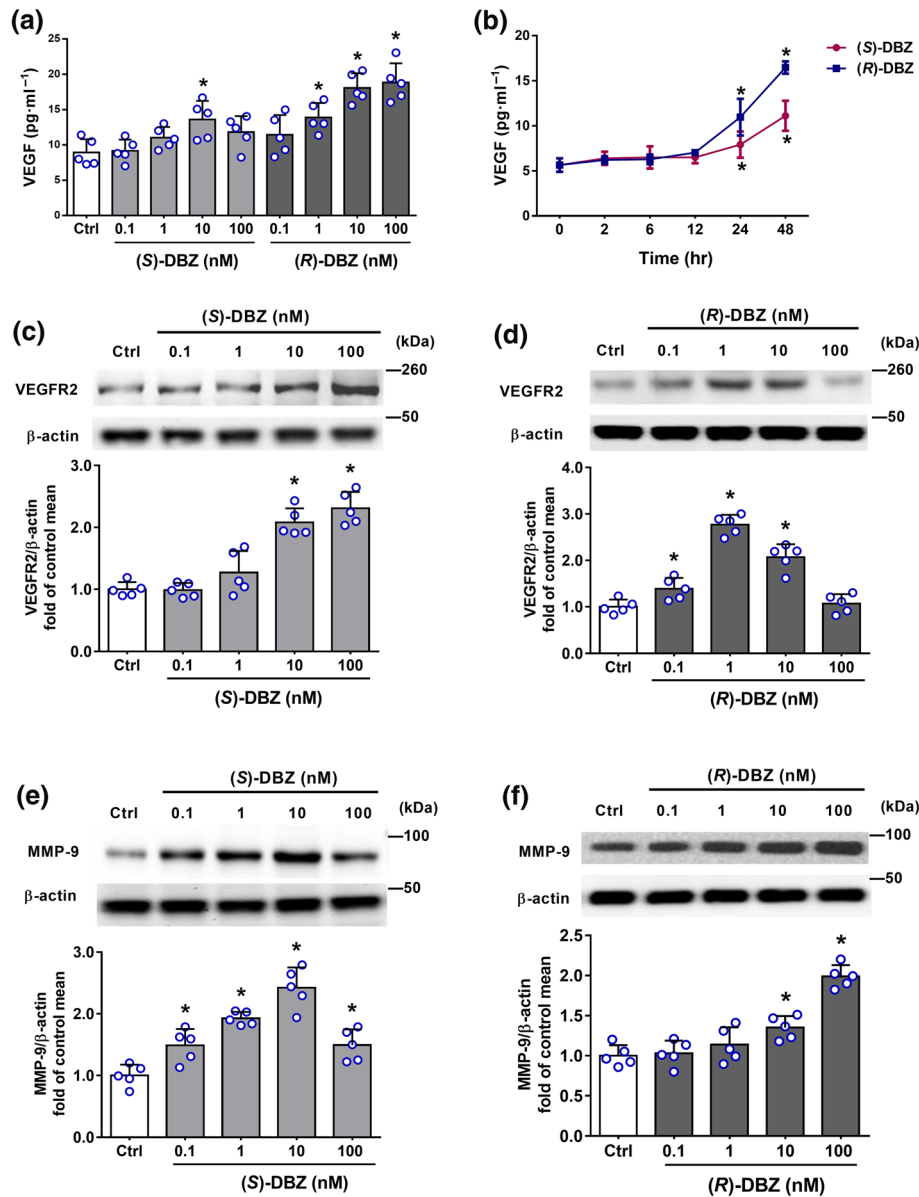


**FIGURE 4** (S)-DBZ and (R)-DBZ increased the expression of VEGF, VEGFR2, and MMP-9. (a) HUVEC were treated with (S)-DBZ and (R)-DBZ respectively at concentrations of 0.1–100 nM for 48 hr; (b) HUVEC were treated with 10-nM (S)-DBZ and (R)-DBZ for 2, 6, 12, 24, and 48 hr; medium was collected and analysed for secreted VEGF level by ELISA. Results are expressed as means  $\pm$  SD ( $n = 5$  independent experiments performed in duplicate). The effects of (S)-DBZ and (R)-DBZ on (c, d) VEGFR2 and (e, f) MMP-9 expression were determined by western blotting assay and quantified by densitometry. Results are expressed as means  $\pm$  SD ( $n = 5$  independent experiments). \* $P < .05$  compared with Ctrl group. Statistical analyses were performed by one-way ANOVA followed by Dunnett's post hoc test or Kruskal-Wallis test with Dunn's post hoc test

In the MAPK signalling pathway, (S)-DBZ increased phosphorylation of PLC $\gamma$  and its downstream target Raf-1 and ERK1/2 in a time-dependent manner (Figure 6a). In (R)-DBZ-treated group, the phosphorylation of PLC $\gamma$  and ERK1/2 peaked at 15 min and dropped at 30 min, and then the phosphorylation increased again, whereas the Raf-1 activation was observed at 5 min with a peak at 15 min and decreasing to near basal levels at 120 min (Figure 6b). On the other hand, phosphorylations of PLC $\gamma$ , Raf-1, and ERK1/2 were enhanced after incubating with different concentrations of (S)-DBZ or (R)-DBZ and up to a peak at 10 nM, respectively (Figure 6c,d).

Furthermore, the phosphorylation of Akt and ERK1/2 induced by (S)-DBZ or (R)-DBZ (10 nM) was abolished after pretreatment with

LY294002 (a PI3K inhibitor) or U0126 (a MEK inhibitor), respectively (Figure 7a–d). Altogether, these results demonstrate that both (S)-DBZ and (R)-DBZ activated PI3K/Akt and MAPK signalling pathways.

### 3.7 | Blockage of the PI3K/Akt or MAPK pathways inhibited the tube formation induced by DBZ

In previous studies, we identified that both (S)-DBZ and (R)-DBZ could activate PI3K/Akt and MAPK pathways. To assess whether Akt and ERK are required for DBZ-induced angiogenesis, cells were pretreated

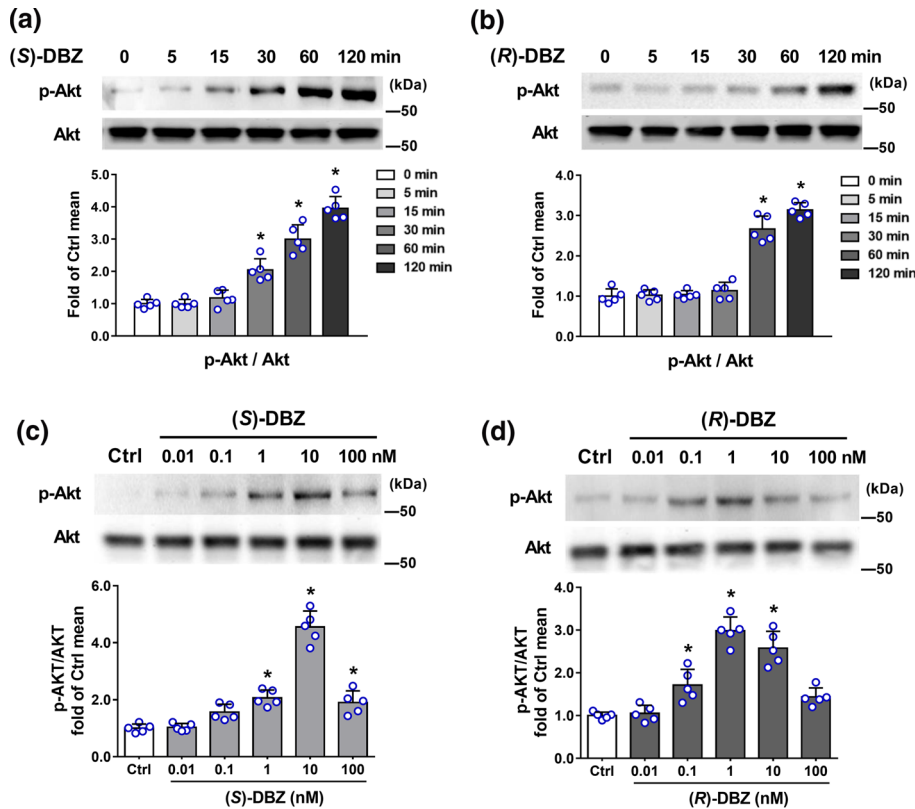


**FIGURE 5** (S)-DBZ and (R)-DBZ increased the phosphorylation of Akt in HUVEC. HUVEC were incubated with (a) (S)-DBZ and (b) (R)-DBZ (10 nM) for the indicated times or with (c) (S)-DBZ and (d) (R)-DBZ in different concentrations for 60 min. Expressions of p-Akt and Akt were analysed by western blotting and quantified by densitometry. Results are expressed as means  $\pm$  SD ( $n = 5$  independent experiments). \* $P < .05$  compared with Ctrl group. Statistical analyses were performed by one-way ANOVA followed by Dunnett's post hoc test

with LY294002 or U0126 for 30 min prior to performing the angiogenesis assays as before. LY294002 or U0126 partially inhibited the tube formation on Matrigel induced by (S)-DBZ or (R)-DBZ, respectively (Figure 7e). Similar results were observed in the HUVEC and HDF co-culture tube formation assay (Figure 7f). These experimental observations demonstrate that Akt and ERK1/2 signalling pathways are critical for DBZ-induced angiogenesis in vitro. Therefore, the network analysis of DBZ based on predicted targets and the experimentally relevant observations validated each other independently (Figure 7g).

### 3.8 | (S)-DBZ and (R)-DBZ attenuated the PTK787-induced inhibition of angiogenesis in zebrafish

Since DBZ enhanced multiple key steps of angiogenesis on endothelial cells in vitro, experiments were performed to determine whether it can promote angiogenesis in vivo. Firstly, we employed Tg (*vegfr2*: GFP) zebrafish embryos for easy monitoring of neovascularization in the ISVs. PTK787 was used to produce a chemically induced blood vessel damage model to investigate the pro-angiogenic effect of DBZ under this circumstance and NBP served as a positive control (Wu et al., 2015; Zhang et al., 2012). As a potent inhibitor of VEGF

receptor TKs, PTK787 displayed an anti-angiogenic property in a dose-dependent manner (Wood et al., 2000). As seen in Figure 8a,b, PTK787 (0.3  $\mu$ M) alone reduced ISV growth. (S)-DBZ in the dose of 5  $\mu$ M administrated with PTK787 significantly rescued ISV formation in zebrafish compared to PTK787 alone group. (R)-DBZ (10  $\mu$ M) also significantly attenuated PTK787-induced blockade of ISV formation in zebrafish. However, neither DSS nor borneol had any effect on the ISVs in zebrafish at the applied doses in PTK787-damaged models (Figure S3).

### 3.9 | DBZ promoted the neovascularization in Matrigel plugs in mice

We performed a mouse Matrigel plug assay to determine whether systemic administration of DBZ exhibits pro-angiogenic effects. The gross view of the plugs harvested after 8 days of implantation showed that nearly transparent grafts in the vehicle-treated control group, while reddish grafts were observed in the DBZ-treated groups (Figure 8c). Quantitative analysis of functioning vessels by haemoglobin determination revealed that DBZ (0.2, 1, and 5  $\text{mg}\cdot\text{kg}^{-1}$ ) produced significant increases in blood content compared with vehicle control, while no significant increase in haemoglobin content at the highest dose (25  $\text{mg}\cdot\text{kg}^{-1}$ ); Matrigel plugs premixed with bFGF and heparin, which

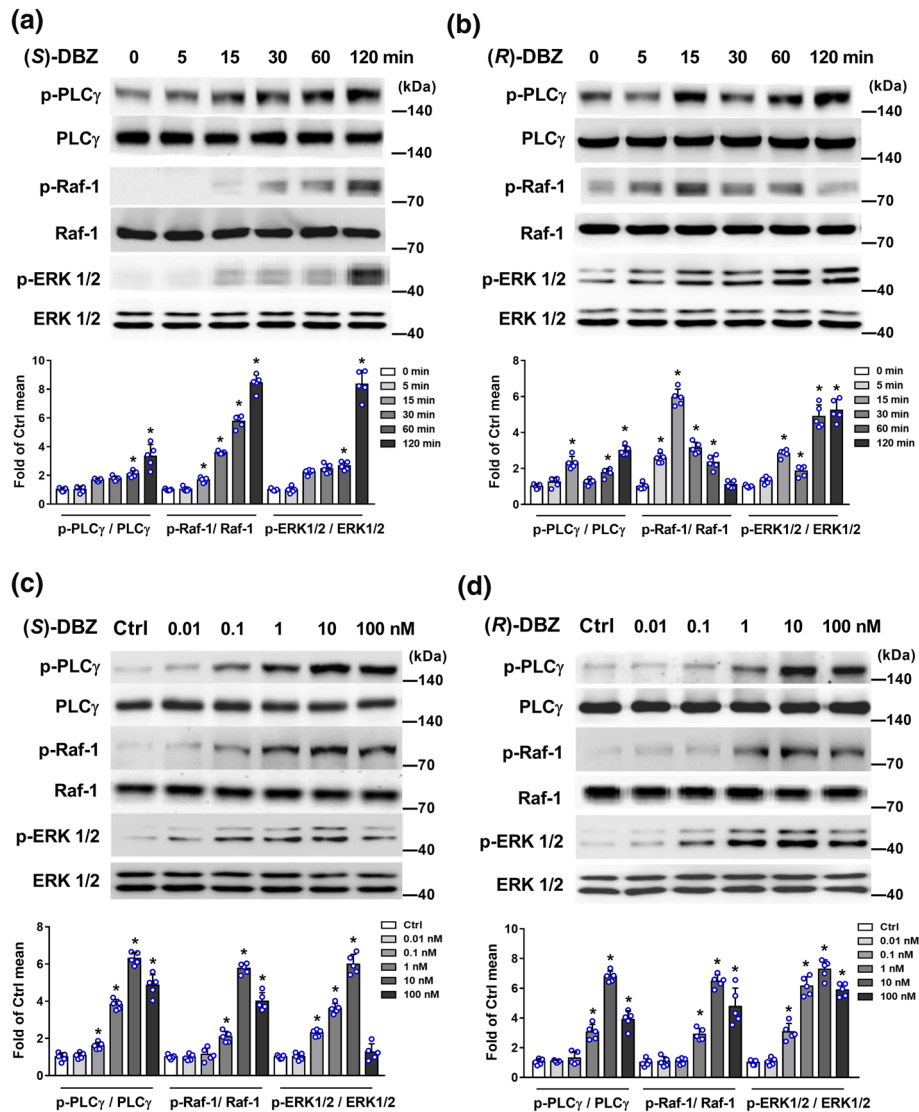


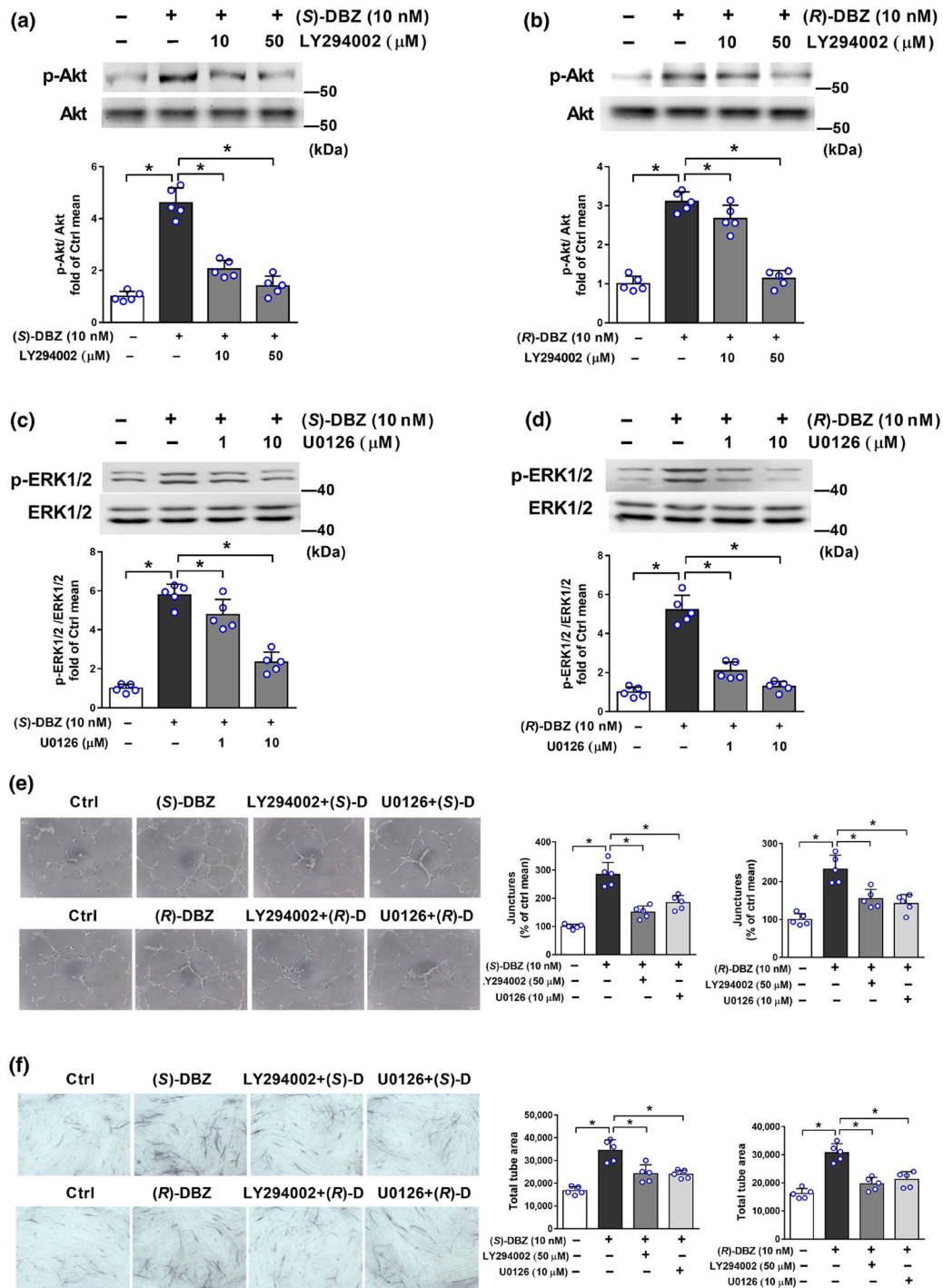
**FIGURE 6** (S)-DBZ and (R)-DBZ activated the MAPK signalling pathways in HUVEC. HUVEC were incubated with (a) (S)-DBZ and (b) (R)-DBZ (10 nM) for the indicated times, or with (c) (S)-DBZ and (d) (R)-DBZ in different concentrations for 60 min. Expressions of p-PLC $\gamma$ , PLC $\gamma$ , p-Raf-1, Raf-1, p-ERK1/2, and ERK1/2 were analysed by western blotting and quantified by densitometry. Results are expressed as means  $\pm$  SD ( $n = 5$  independent experiments). \* $P < .05$  compared with Ctrl group. Statistical analyses were performed by one-way ANOVA followed by Dunnett's post hoc test or Kruskal–Wallis test with Dunn's post hoc test

served as a positive control, induced a strongest angiogenic reaction (Figure 8d). Histological analyses via H&E staining showed that almost no vessel-like structures were observed in the vehicle control group; newly formed vessels and vessel-like structures, as well as blood vessels containing red blood cells (yellow arrowheads) were clearly visible in DBZ-treated groups and positive control group (Figure 8e). Notably, haemorrhage was shown in positive control plugs by the numerous undefined borders of the vessels and extravascular red blood cells, which revealed that the vessels treated with bFGF and heparin are leaky. In addition, the neovascularization promoted by DBZ treatment was confirmed by immunostaining for CD31, an endothelial marker (Figure 8f,g). Taken together, these data identify DBZ as a novel small molecule angiogenesis stimulator that functions both in vivo and in vitro.

## 4 | DISCUSSION

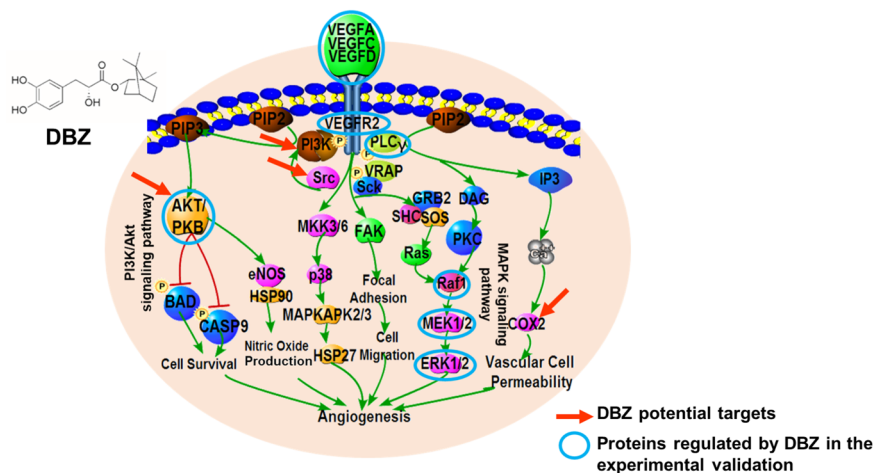
Here, we show for the first time that the novel synthetic compound DBZ promoted angiogenesis both in vitro and in vivo. Mechanistically, the DBZ-induced activation of Akt and ERK1/2 as well as the angiogenic process were abolished by the PI3K and MEK inhibitors, respectively, suggesting that the PI3K/Akt and PLC $\gamma$ /Raf-1/MEK/ERK signalling pathways play critical roles in DBZ-induced angiogenesis. In the present study, differential effects of the two DBZ isomers on angiogenesis were also observed, especially on cell proliferation, VEGF secretion, MAPK pathway activation, and tube formation in co-culture models, with (R)-DBZ being more potent than (S)-DBZ. Therefore, it is attractive to further explore the pharmacological differences and underlying mechanism between the two isomers of DBZ.





**FIGURE 7** Effect of PI3K inhibitor LY294002 and MEK1/2 inhibitor U0126 on DBZ-induced angiogenesis. HUVEC were pretreated with the indicated inhibitors for 30 min before the addition of (S)-DBZ or (R)-DBZ (10 nM). After another 60-min incubation, the levels of phosphorylated and total (a, b) Akt or (c, d) ERK1/2 were detected by western blotting. Results are expressed as means  $\pm$  SD ( $n = 5$  independent experiments). (e) Matrigel tube formation was measured in HUVEC incubated with (S)-DBZ or (R)-DBZ (10 nM) for 6 hr. (f) Tube formation was measured in HUVEC-HDF co-culture system stimulated with (S)-DBZ or (R)-DBZ (10 nM) that were pretreated with LY294002 or U0126. Results are expressed as means  $\pm$  SD ( $n = 5$  independent experiments performed in triplicate for Matrigel assays;  $n = 5$  independent experiments with five wells each for co-culture assays). \* $P < .05$  versus (S)-DBZ or (R)-DBZ. Statistical analyses were performed by one-way ANOVA followed by Dunnett's post hoc test. (g) DBZ can regulate proteins in the VEGF-related signalling pathway. Red arrows point to potential targets of DBZ identified by in silico prediction, and some key proteins (blue circles) in the VEGF-related signalling pathway were validated experimentally

(g)


**FIGURE 7** Continued

As we know, VEGF plays the most prominent role in initiating the process of angiogenesis. Therefore, it is interesting to explore whether the pro-angiogenic effects of DBZ is VEGF dependent. On the one hand, although we observed DBZ-induced increase of VEGF secretion by HUVEC, it occurred only with prolonged treatment up to 24 hr. On the other hand, our findings that DBZ rapidly induced activation of Akt and MAPK pathways suggest a non-genomic rather than genomic action. Moreover, data from our wound healing assay (8 hr), transwell assay (4 hr), as well as Matrigel tube formation assay (6 hr) all indicated that DBZ could promote endothelial cell migration and tube formation many hours before inducing VEGF secretion. Thus, the above findings indicate that DBZ could exert its angiogenic effect through a VEGF-independent mechanism.

To investigate the angiogenic activity of DBZ *in vivo*, we used a transgenic zebrafish model expressing GFP under the control of the VEGF receptor 2 promoter (*vegfr2: GFP*; Cross, Cook, Lin, Chen, & Rubinstein, 2003). Zebrafish as a model organism exhibits genetic and functional conservation across angiogenic pathways. The major modulators of angiogenesis and tyrosine-kinase domains of VEGFR2 are conserved (Chan, Bayliss, Wood, & Roberts, 2002; Liang et al., 2001). Thus, the potent VEGFR TK inhibitor PTK787 was used in zebrafish model, which inhibited autophosphorylation of kinase insert domain-containing receptor and therefore effectively blocked angiogenesis (Bayliss et al., 2006; Wood et al., 2000). When the VEGFR was impaired, the downstream component may stay at low activity. This well-established chemically induced blood vessel damage model can also mimic certain pathological conditions relating to angiogenesis deficiencies (Mu et al., 2017; Wu et al., 2015). It was found that DBZ could partially restore PTK787-induced blockade of ISV formation in zebrafish. This observation can either be interpreted as DBZ's pro-angiogenic activity or protective effect against vascular disruption induced by PTK787. Chan et al. reported that the PTK787-induced VEGFR defect can be ameliorated by up-regulating the activity of a downstream effector Akt, allowing for normal endothelial cell functions in migration and survival (Chan et al., 2002). Besides, they observed a modest rescue in the number of ISVs in zebrafish in the

presence of PTK787 by activating Akt downstream element eNOS (Chan et al., 2002). Similarly, DBZ, which can activate Akt pathway in HUVECs, allowed blood vessels to form in the presence of PTK787. Therefore, we hypothesize that DBZ rescue the chemically induced VEGFR defect in zebrafish by activating a downstream effector of VEGF signalling.

Notably, there is a discrepancy of DBZ effective concentrations between *in vitro* and zebrafish assays. We speculate that the different sensitivity to DBZ may be partially due to the damaged vessel model we used in the zebrafish assay. In addition, it is worthy of note that the zebrafish model used in this study is based on embryonic development, and both zebrafish model and mouse Matrigel plug model are not a real pathology model. Thus, further study on more relevant pathological vascular injury model or ischaemic model is required for investigating the equilibrium effect and effective doses of DBZ on angiogenesis *in vivo*.

Imbalance in the angiogenic and anti-angiogenic mediators triggers angiogenesis, which may be physiological in the normal state or pathological as in atherosclerosis. Physiological angiogenesis is instrumental for restoration of vessel wall normoxia and resolution inflammation, leading to atherosclerosis regression (Moreno, Sanz, & Fuster, 2009). However, pathological angiogenesis plays a role in atherosclerotic plaque growth and instability (Moreno, Purushothaman, Sirol, Levy, & Fuster, 2006; Caroline Camaré, Pucelle, Nègre-Salvayre, & Salvayre, 2017). *In vivo* Matrigel assays showed that systemic administration of DBZ at low doses (0.2, 1, and 5 mg·kg<sup>-1</sup>·day<sup>-1</sup>) induced vascularization in Matrigel plug in C57BL/6 mice (Figure 8c–g). Interestingly, we also found DBZ (20 and 40 mg·kg<sup>-1</sup>·day<sup>-1</sup>) markedly reduced atherosclerotic lesion formation and attenuated the progression of pre-established atherosclerotic plaques in ApoE<sup>-/-</sup> mice by inhibiting inflammation, macrophage migration, leukocyte adhesion, and foam cell formation (Wang et al., 2017). The discrepancy between DBZ's pro-angiogenic effect and anti-atherosclerosis effect is very likely to be due to a dose-dependent pleiotropic modulation in response to different microenvironments and ongoing pathophysiology. This postulate is also supported by the differential effects of DBZ on

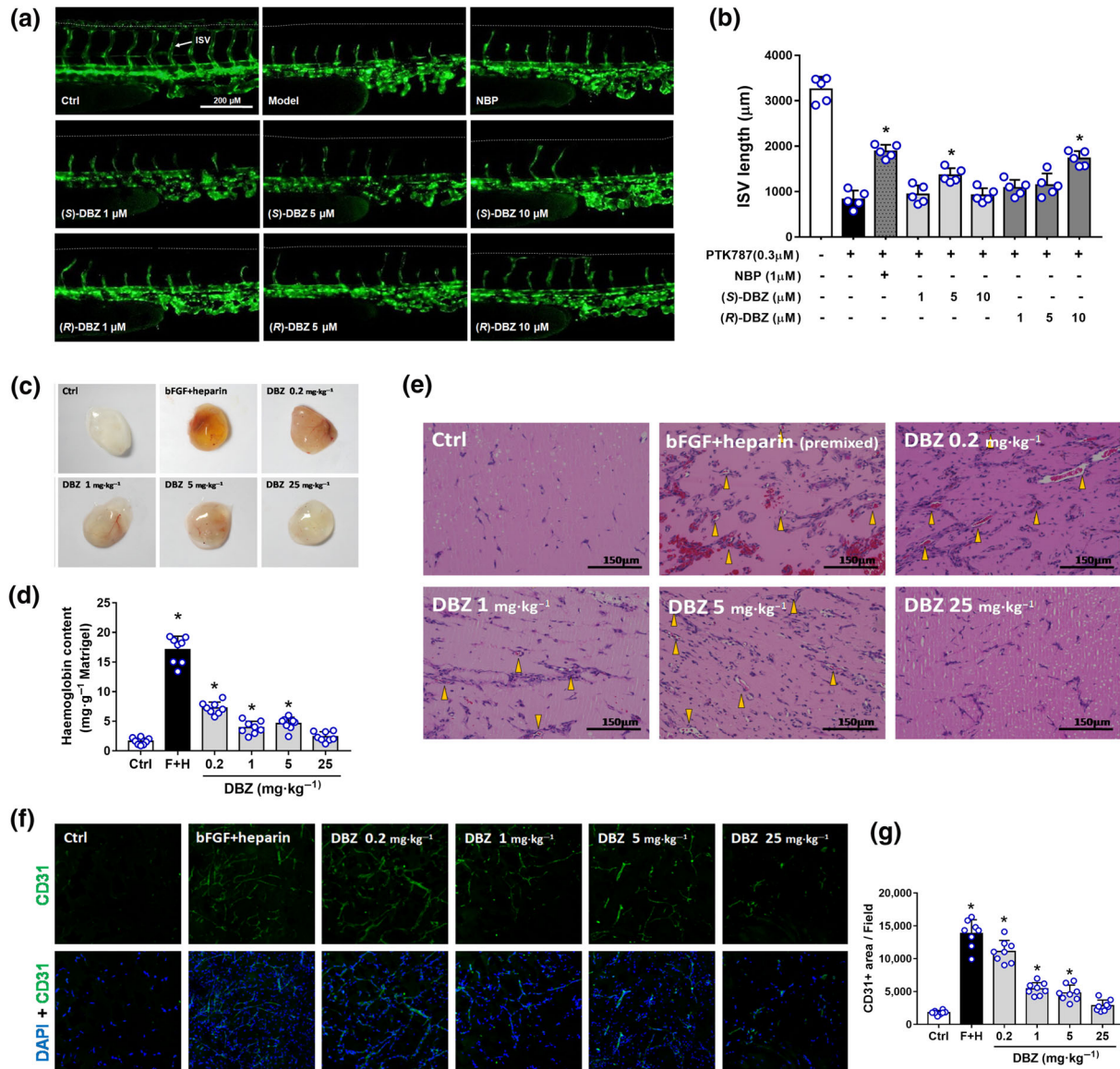


**FIGURE 8** DBZ restored the PTK787-induced ISV angiogenesis impairment in zebrafish embryos (a, b) and promoted vascularization in Matrigel plugs in mice (c–g). (a) Lateral view of vehicle control embryos and embryos treated with PTK787, PTK787 with NBP, PTK787 with (S)-DBZ (1, 5, and 10  $\mu\text{M}$ ), and PTK787 with (R)-DBZ (1, 5, and 10  $\mu\text{M}$ ) for 24 hr. NBP was used as a positive control. ISVs are indicated by the white arrows. (b) Quantification of total length of ISVs induced by (S)-DBZ and (R)-DBZ. Data are presented as the means  $\pm$  SD (10 fish embryos per well from five time-independent experiments;  $n = 5$ ). Statistical analyses were performed by one-way ANOVA followed by Dunnett's post hoc test.  $^*P < .05$  versus PTK787-treated group. NBP, butylphthalide. (c) Representative pictures of Matrigel plugs. Matrigel premixed with bFGF (150  $\text{ng}\cdot\text{ml}^{-1}$  in PBS) plus heparin (64  $\text{u}\cdot\text{ml}^{-1}$  in PBS) (F + H, positive control), or containing the same volume of PBS alone, was injected s.c. into C57BL/6 mice. Vehicle and DBZ (0.2, 1, 5, or 25  $\text{mg}\cdot\text{kg}^{-1}\cdot\text{day}^{-1}$ ) were administered i.p. Plugs were removed after 8 days and photographed. (d) Haemoglobin levels in the Matrigel plug were quantified using the Drabkin reagent kit and were normalized to the plug weight. Data are presented as the means  $\pm$  SD ( $n = 8$  plugs from eight mice per group). (e) Sections of Matrigel plugs were stained by H&E and photographed. The yellow arrowhead shows blood vessels containing red blood cells. The scale bar represents 150  $\mu\text{m}$ . (f) Representative immunofluorescence images of Matrigel plug sections labelled with anti-CD31 antibody and counterstained with DAPI (magnification: 200 $\times$ ). (g) Quantification of CD31+ area of new microvessels show that DBZ (0.2, 1, and 5  $\text{mg}\cdot\text{kg}^{-1}\cdot\text{day}^{-1}$ ) increased microvessel formation significantly compared with the vehicle control. Data are presented as the means  $\pm$  SD ( $n = 8$  mice per group). Statistical analyses were performed by one-way ANOVA followed by Dunnett's post hoc test or unpaired  $t$  test with Welch's correction.  $^*P < .05$  versus vehicle control group

endothelial cells and monocytes at different concentration ranges in vitro. At relatively low concentrations of  $10^{-9}$  to  $10^{-7}$  M, DBZ produced an angiogenic phenotype in human endothelial cells. However, at higher concentrations of  $5\text{--}20 \times 10^{-6}$  M, DBZ inhibited atherosclerosis by suppressing LPS-stimulated macrophages migration and

oxidized LDL-induced foam cell formation (Wang et al., 2017). Besides, DBZ showed significant protective effects on vascular endothelial cell viability and tube formation against Hcy-induced injury (Figure S2A–D), which has beneficial effect on atherosclerosis as well. Interestingly, statins, the gold standard for preventing and treating



atherosclerotic cardiovascular diseases, also has other benefits (e.g., angiogenic modulating effects) apart from their lipid-lowering effects (Elewa, Elremessy, Somanath, & Fagan, 2010). It has a biphasic dose-dependent effect on angiogenesis characterized by a pro-angiogenic effect at low doses and anti-angiogenic effect at high doses (Katsumoto et al., 2005; Skaletz-Rorowski & Walsh, 2003; Zhu et al., 2008). Similar case was showed in ginsenoside 20(R)-Rg<sub>3</sub>, which reduced angiogenic activity of HUVEC at nanomolar level, whereas induced angiogenesis at micromolar level (Kwok et al., 2012). It is not surprising that a single compound can act on different targets at different concentrations. Genistein, the soy phytoestrogen, can activate oestrogen receptor at low concentration (<mM) and inhibit adipogenesis; however, at high concentration (>mM), it promotes adipogenesis through acting as a ligand of PPAR $\gamma$  (Dang, Audinot, Papapoulos, Boutin, & Löwik, 2003). Therefore, we supposed that the pleiotropic activity of DBZ at low and high doses may be due to the different targets involved.

As we know, many single herbal compounds target multiple components of the dysregulated network of genes involved in diseases, leading to multiple pharmacological activities resulting from different molecular mechanisms. The potential targets of DBZ by *in silico* study not only revealed an effect on angiogenesis but also identified, previously observed, multiple pharmacological activities of DBZ. In our previous studies, DBZ was found to be a PPAR $\gamma$  agonist, by *in silico* prediction (PPAR $\gamma$  was ranked in the top 5% in the target list of DBZ), which was validated experimentally (Xu et al., 2017). In this study, for instance, based on our predicted results, we also found that the platelet activation pathway was involved and P2Y<sub>12</sub> receptors (P2RY12) were ranked in the top 5% in the target list of DBZ. Thus, it would be interesting to further explore its effect on platelet aggregation and thrombosis.

Inspired by the combinatorial therapy and the successful use of composite Danshen formulations in the clinic, DBZ was designed by the chemical combination of DSS and borneol (Figure S1). Co-culture data showed that DSS only at 1 nM induced tube formation and borneol exerted no effect, whereas both (S)-DBZ and (R)-DBZ were more potent in promoting tube formation than the parent compounds. Moreover, an *in vivo* study also revealed that (S)-DBZ and (R)-DBZ could reverse PTK787-induced inhibition of angiogenesis (or vascular disruption) in zebrafish embryos, whereas DSS or borneol exerted no such effect. All these findings strongly indicate that DBZ is biochemically and functionally distinct from its parent compounds. Besides the promoting effect of borneol on bioavailability, one difference between DBZ and DSS in structure is that DBZ is composed of one phenolic ring and a C-6 ring linked by an ester bond, whereas DSS is a phenolic compound only. We infer that the conjugated form of phenolic ring from DSS with C-6 ring from borneol linked by ester bond may be critical in DBZ-induced pro-angiogenic activity. Therefore, the relationship between the structure and biological differences of DSS and DBZ needs to be further elucidated.

This study revealed, for the first time, that the two isomers of the novel compound DBZ can induce key features of angiogenesis *in vitro*, including endothelial cell proliferation, migration, and tube formation,

and at least in part through activating Akt and MAPK signalling pathways. Further studies are still needed to explore and verify the direct targets and other signalling pathways involved in DBZ-induced angiogenesis. It is remarkable that both (S)-DBZ and (R)-DBZ were not only more potent in promoting vascular tube formation *in vitro* than their parent compounds (i.e., DSS and borneol) but could also reverse PTK787-induced inhibition of angiogenesis (or vascular disruption) and promote neovascularization in mice Matrigel plugs *in vivo*. Predicted by network target analysis and validated experimentally, DBZ has been confirmed as a unique angiogenesis stimulator. Collectively, these data suggest that it has the potential to be developed further for treating myocardial infarction, stroke, and other cardiovascular diseases.

## ACKNOWLEDGEMENTS

This work was supported by grants from the National Natural Science Foundation of China (81630103 and 81225025), the Primary R&D Plan of Shaanxi Province (2017KW-055 and 2018SF-293), the Scientific Research Plan Projects of Shaanxi Provincial Education Department (17JK0764), the National College Students Innovation and Entrepreneurship Training Project (201810697021), the National Key Scientific Instrument and Equipment Development Project of China (2013YQ170525), Changjiang Scholars and Innovative Research Team in University (IRT\_15R55), and Opening Foundation of Key Laboratory of Resource Biology and Biotechnology in Western China (Northwest University), Ministry of Education.

## CONFLICT OF INTEREST

The authors declare no conflicts of interest.

## AUTHOR CONTRIBUTIONS

TP.F. and XH.Z. designed the projects; S.L., JN.W., JX.S., RM.L., YL.F., and XM.K. performed the *in vitro* experiments and participated in statistical analysis; S.L. wrote the manuscript; LW.H. and KC.L. performed the zebrafish experiments; S.L., JN.W., and RM.L. performed the Matrigel plug assays; X.W., P.Z., and S.L. performed the *in silico* prediction and network analysis experiments; TP.F., S.L., and XP.Z. reviewed and edited the paper. All authors agreed on the final version.

## DECLARATION OF TRANSPARENCY AND SCIENTIFIC RIGOUR

This Declaration acknowledges that this paper adheres to the principles for transparent reporting and scientific rigour of preclinical research as stated in the *BJP* guidelines for [Design & Analysis](#), [Immunoblotting and Immunochimistry](#), and [Animal Experimentation](#), and as recommended by funding agencies, publishers and other organisations engaged with supporting research.

## ORCID

Sha Liao  <https://orcid.org/0000-0001-5825-5514>

Xiaohui Zheng  <https://orcid.org/0000-0001-5672-3134>



## REFERENCES

- Alexander, S. P., Fabbro, D., Kelly, E., Marrion, N. V., Peters, J. A., Faccenda, E., ... CGTP Collaborators. (2017a). The Concise Guide to PHARMACOLOGY 2017/18: Catalytic receptors. *British Journal of Pharmacology*, 174, S225–S271. <https://doi.org/10.1111/bph.13876>
- Alexander, S. P., Fabbro, D., Kelly, E., Marrion, N. V., Peters, J. A., Faccenda, E., ... CGTP Collaborators. (2017b). The Concise Guide to PHARMACOLOGY 2017/18: Enzymes. *British Journal of Pharmacology*, 174, S272–S359. <https://doi.org/10.1111/bph.13877>
- Bai, Y., Zhang, Q., Jia, P., Yang, L., Sun, Y., Nan, Y., ... Zheng, X. (2014). Improved process for pilot-scale synthesis of Danshensu ((±)-DSS) and its enantiomer derivatives. *Organic Process Research & Development*, 18, 1667–1673. <https://doi.org/10.1021/op4002593>
- Barabási, A. L., Gulbahce, N., & Loscalzo, J. (2011). Network medicine: A network-based approach to human disease. *Nature Reviews Genetics*, 12, 56–68. <https://doi.org/10.1038/nrg2918>
- Bayliss, P. E., Bellavance, K. L., Whitehead, G. G., Abrams, J. M., Aegerter, S., Robbins, H. S., ... Chan, J. (2006). Chemical modulation of receptor signaling inhibits regenerative angiogenesis in adult zebrafish. *Nature Chemical Biology*, 2, 265–273. <https://doi.org/10.1038/nchembio778>
- Besnard, J., Ruda, G. F., Setola, V., Abecassis, K., Rodriguez, R. M., Huang, X. P., ... Hopkins, A. L. (2012). Automated design of ligands to polypharmacological profiles. *Nature*, 492, 215–220. <https://doi.org/10.1038/nature11691>
- Bishop, E. T., Bell, G. T., Bloor, S., Broom, I. J., Hendry, N. F. K., & Wheatley, D. N. (1999). An in vitro model of angiogenesis: Basic features. *Angiogenesis*, 3, 335–344. <https://doi.org/10.1023/A:1026546219962>
- Briggs, J. (2014). A global scientific challenge: Learning the right lessons from ancient healing practices. *Science*, 346(6216 Suppl), S7–S9.
- Cai, Z., Hou, S., Li, Y., Zhao, B., Yang, Z., Xu, S., & Pu, J. (2008). Effect of borneol on the distribution of gastrodin to the brain in mice via oral administration. *Journal of Drug Targeting*, 16, 178–184. <https://doi.org/10.1080/10611860701794395>
- Cannon, J. E., Upton, P. D., Smith, J. C., & Morrell, N. W. (2010). Intersegmental vessel formation in zebrafish: Requirement for VEGF but not BMP signalling revealed by selective and non-selective BMP antagonists. *British Journal of Pharmacology*, 161, 140–149. <https://doi.org/10.1111/j.1476-5381.2010.00871.x>
- Caroline Camaré, C., Pucelle, M., Nègre-Salvayre, A., & Salvayre, R. (2017). Angiogenesis in the atherosclerotic plaque. *Redox Biology*, 12, 18–34. <https://doi.org/10.1016/j.redox.2017.01.007>
- Chan, J., Bayliss, P. E., Wood, J. M., & Roberts, T. M. (2002). Dissection of angiogenic signaling in zebrafish using a chemical genetic approach. *Cancer Cell*, 1(3), 257–267. [https://doi.org/10.1016/S1535-6108\(02\)00042-9](https://doi.org/10.1016/S1535-6108(02)00042-9)
- Chan, K., Chui, S. H., Wong, D. Y. L., Ha, W. Y., Chan, C. L., & Wong, R. N. S. (2004). Protective effects of Danshensu from the aqueous extract of *Salvia miltiorrhiza* (Danshen) against homocysteine-induced endothelial dysfunction. *Life Sciences*, 75, 3157–3171. <https://doi.org/10.1016/j.lfs.2004.06.010>
- Chen, T. F., Lin, S. G., Chen, L. X., Jiang, G. F., Liang, Z. Y., Yang, M., ... Xie, Y. A. (1990). Enhancement of absorption of tetramethylpyrazine by synthetic borneol. *Acta Pharmacologica Sinica*, 11, 42–44.
- Cross, L. M., Cook, M. A., Lin, S., Chen, J. N., & Rubinstein, A. L. (2003). Rapid analysis of angiogenesis drugs in a live fluorescent zebrafish assay. *Arteriosclerosis, Thrombosis, and Vascular Biology*, 23, 911–912. <https://doi.org/10.1161/01.ATV.0000068685.72914.7E>
- Curtis, M. J., Alexander, S., Cirino, G., Docherty, J. R., George, C. H., Giembycz, M. A., ... Ahluwalia, A. (2018). Experimental design and analysis and their reporting II: updated and simplified guidance for authors and peer reviewers. *British Journal of Pharmacology*, 175(7), 987–993. <https://doi.org/10.1111/bph.14153>
- Dang, Z. C., Audinot, V., Papapoulos, S. E., Boutin, J. A., & Löwik, C. W. (2003). Peroxisome proliferator-activated receptor  $\gamma$  (PPAR $\gamma$ ) as a molecular target for the soy phytoestrogen genistein. *Journal of Biological Chemistry*, 278(2), 962–967. <https://doi.org/10.1074/jbc.M209483200>
- Dong, C., Wang, Y., & Zhu, Y. Z. (2009). Asymmetric synthesis and biological evaluation of Danshensu derivatives as anti-myocardial ischemia drug candidates. *Bioorganic & Medicinal Chemistry*, 17, 3499–3507. <https://doi.org/10.1016/j.bmc.2009.02.065>
- Elewa, H. F., Elremessy, A. B., Somanath, P. R., & Fagan, S. C. (2010). Diverse effects of statins on angiogenesis: New therapeutic avenues. *Pharmacotherapy*, 30(2), 169–176.
- Hanahan, D., & Folkman, J. (1996). Patterns and emerging mechanisms of the angiogenic switch during tumorigenesis. *Cell*, 86, 353–364. [https://doi.org/10.1016/S0092-8674\(00\)80108-7](https://doi.org/10.1016/S0092-8674(00)80108-7)
- Harding, S. D., Sharman, J. L., Faccenda, E., Southan, C., Pawson, A. J., Ireland, S., ... NC-IUPHAR. (2018). The IUPHAR/BPS guide to pharmacology in 2018: Updates and expansion to encompass the new guide to immunopharmacology. *Nucl Acids Res*, 46, D1091–D1106. <https://doi.org/10.1093/nar/gkx1121>
- Hoeben, A., Landuyt, B., Highley, M. S., Wildiers, H., Van Oosterom, A. T., & De Buijn, E. A. (2004). Vascular endothelial growth factor and angiogenesis. *Pharmacological Reviews*, 56, 549–580. <https://doi.org/10.1124/pr.56.4.3>
- Huang, d. W., Sherman, B. T., & Lempicki, R. A. (2009). Systematic and integrative analysis of large gene lists using DAVID bioinformatics resources. *Nature Protocols*, 4, 44–57. <https://doi.org/10.1038/nprot.2008.211>
- Jain, R. K., Schlenger, K., Hockel, M., & Yuan, F. (1997). Quantitative angiogenesis assays: Progress and problems. *Nature Medicine*, 3(11), 1203–1208. <https://doi.org/10.1038/nm1197-1203>
- Katsumoto, M., Shingu, T., Kuwashima, R., Nakata, A., Nomura, S., & Chayama, K. (2005). Biphasic effect of HMG-CoA reductase inhibitor, pitavastatin, on vascular endothelial cells and angiogenesis. *Circulation Journal*, 69(12), 1547–1555. <https://doi.org/10.1253/circj.69.1547>
- Kilkenny, C., Browne, W., Cuthill, I. C., Emerson, M., & Altman, D. G. (2010). Animal research: Reporting in vivo experiments: the ARRIVE guidelines. *Br J Pharmacol*, 160, 1577–1579.
- Kwok, H. H., Guo, G. L., Lau, K. C., Cheng, Y. K., Wang, J. R., Jiang, Z. H., ... Wong, R. N. (2012). Stereoisomers ginsenosides-20(S)-Rg3 and -20(R)-Rg3 differentially induce angiogenesis through peroxisome proliferator-activated receptor- $\gamma$ . *Biochemical Pharmacology*, 83(7), 893–902. <https://doi.org/10.1016/j.bcp.2011.12.039>
- Lauder, H., Frost, E. E., Hiley, C. R., & Fan, T. P. (1998). Quantification of the repair process involved in the repair of a cell monolayer using an in vitro model of mechanical injury. *Angiogenesis*, 2, 67–80.
- Leung, K., Cheung, L., Pon, Y., Wong, R., Mak, N., Fan, T. P., ... Wong, A. S. (2007). Ginsenoside Rb1 inhibits tube-like structure formation of endothelial cells by regulating pigment epithelium-derived factor through the oestrogen  $\beta$  receptor. *British Journal of Pharmacology*, 152(2), 207–215. <https://doi.org/10.1038/sj.bjp.0707359>
- Li, S., & Zhang, B. (2013). Traditional Chinese medicine network pharmacology: Theory, methodology and application. *Chinese Journal of Natural Medicines*, 11(2), 110–120. [https://doi.org/10.1016/S1875-5364\(13\)60037-0](https://doi.org/10.1016/S1875-5364(13)60037-0)
- Liang, D., Chang, J. R., Chin, A. J., Smith, A., Kelly, C., Weinberg, E. S., & Ge, R. (2001). The role of vascular endothelial growth factor (VEGF) in vasculogenesis, angiogenesis, and hematopoiesis in zebrafish development. *Mechanisms of Development*, 108, 29–43. [https://doi.org/10.1016/S0925-4773\(01\)00468-3](https://doi.org/10.1016/S0925-4773(01)00468-3)
- Liang, X., Li, H., & Li, S. (2014). A novel network pharmacology approach to analyze traditional herbal formulae: The Liu-Wei-Di-Huang pill as a case study. *Molecular BioSystems*, 10(5), 1014–1022. <https://doi.org/10.1039/C3MB70507B>
- Liu, J., Li, X., Hu, S. S., Yu, Q. L., Sun, W. J., & Zheng, X. H. (2008). Studies on the effects of Baras Camphor on the tissue distribution of *Salvia miltiorrhiza* Bge. In complex Danshen prescription in rabbits. *Chinese Journal of Pharmaceutical Analysis*, 28(10), 1612–1615.

- Lu, T., Yang, J., Gao, X., Chen, P., Du, F., Sun, Y., ... Li, C. (2008). Plasma and urinary tanshinol from *Salvia miltiorrhiza* (Danshen) can be used as pharmacokinetic markers for cardiotoxic pills, a cardiovascular herbal medicine. *Drug Metabolism & Disposition the Biological Fate of Chemicals*, 36, 1578–1586. <https://doi.org/10.1124/dmd.108.021592>
- Moreno, P. R., Purushothaman, K. R., Sirol, M., Levy, A. P., & Fuster, V. (2006). Neovascularization in human atherosclerosis. *Circulation*, 113(18), 2245–2252. <https://doi.org/10.1161/CIRCULATIONAHA.105.578955>
- Moreno, P. R., Sanz, J., & Fuster, V. (2009). Promoting mechanisms of vascular health: Circulating progenitor cells, angiogenesis, and reverse cholesterol transport. *Journal of the American College of Cardiology*, 53(25), 2315–2323. <https://doi.org/10.1016/j.jacc.2009.02.057>
- Mu, X. M., Zhao, T., Xu, C., Shi, W., Geng, B., Shen, J. J., ... You, Q. (2017). Oncometabolite succinate promotes angiogenesis by upregulating VEGF expression through GPR91-mediated STAT3 and ERK activation. *Oncotarget*, 8(8), 13174–13185. <https://doi.org/10.18632/oncotarget.14485>
- Murray, C. J. (2001). *Methods in molecular medicine: Angiogenesis protocols*. Totowa, NJ: Humana Press.
- Newman, D. J., & Cragg, G. M. (2016). Natural products as sources of new drugs from 1981 to 2014. *Journal of Natural Products*, 79(3), 629–661. <https://doi.org/10.1021/acs.jnatprod.5b01055>
- Nowak-Sliwinska, P., Alitalo, K., Allen, E., Anisimov, A., Aplin, A. C., Auerbach, R., ... Griffioen, A. W. (2018). Consensus guidelines for the use and interpretation of angiogenesis assays. *Angiogenesis*, 21(3), 425–532. <https://doi.org/10.1007/s10456-018-9613-x>
- Qiu, J. (2007). Traditional medicine: A culture in the balance. *Nature*, 448, 126–128. <https://doi.org/10.1038/448126a>
- Sengupta, S., Toh, S. A., Sellers, L. A., Skepper, J. N., Koolwijk, P., Leung, H. W., ... Fan, T. P. D. (2004). Modulating angiogenesis: The yin and the yang in ginseng. *Circulation*, 110(10), 1219–1225. <https://doi.org/10.1161/01.CIR.0000140676.88412.CF>
- Skaletz-Rorowski, A., & Walsh, K. (2003). Statin therapy and angiogenesis. *Current Opinion in Lipidology*, 14(6), 599–603. <https://doi.org/10.1097/00041433-200312000-00008>
- Staton, C. A., Lewis, C. E., & Bicknell, R. (2007). *Angiogenesis assays: A critical appraisal of current techniques*. Chippingham, Wilts: Wiley.
- Tirziu, D., & Simons, M. (2005). Angiogenesis in the human heart: Gene and cell therapy. *Angiogenesis*, 8, 241–251. <https://doi.org/10.1007/s10456-005-9011-z>
- Wang, J., Xu, P. F., Xie, X. N., Li, J., Zhang, J., Wang, J. L., ... Zhai, Y. (2017). DBZ (Danshensu Bingpian Zhi), a novel natural compound derivative, attenuates atherosclerosis in apolipoprotein E-deficient mice. *Journal of the American Heart Association*, 6, e006297.
- Wang, L., Zhou, G. B., Liu, P., Song, J. H., Liang, Y., Yan, X. J., ... Chen, Z. (2008). Dissection of mechanisms of Chinese medicinal formula Realgar-Indigo naturalis as an effective treatment for promyelocytic leukemia. *Proceedings of the National Academy of Sciences*, 105, 4826–4831. <https://doi.org/10.1073/pnas.0712365105>
- Wood, J. M., Bold, G., Buchdunger, E., Cozens, R., Ferrari, S., Frei, J., ... Totzke, F. (2000). PTK787/ZK 222584, a novel and potent inhibitor of vascular endothelial growth factor receptor tyrosine kinases, impairs vascular endothelial growth factor-induced responses and tumor growth after oral administration. *Cancer Research*, 60, 2178–2189.
- Wu, F., Song, H., Zhang, Y., Zhang, Y., Mu, Q., Jiang, M., ... Tang, D. (2015). Irisin induces angiogenesis in human umbilical vein endothelial cells in vitro and in zebrafish embryos in vivo via activation of the ERK signaling pathway. *PLoS ONE*, 10(8), e0134662. <https://doi.org/10.1371/journal.pone.0134662>
- Xu, P. F., Hong, F., Wang, J. L., Wang, J., Zhao, X., Wang, S., ... Zhai, Y. (2017). DBZ is a putative PPAR $\gamma$  agonist that prevents high fat diet-induced obesity, insulin resistance and gut dysbiosis. *Biochimica et Biophysica Acta (BBA)-General Subjects*, 1861(11 Pt A), 2690–2701. <https://doi.org/10.1016/j.bbagen.2017.07.013>
- Yang, H., Xun, Y., Li, Z., Hang, T., Zhang, X., & Cui, H. (2009). Influence of borneol on in vitro corneal permeability and on in vivo and in vitro corneal toxicity. *Journal of International Medical Research*, 37, 791–802. <https://doi.org/10.1177/147323000903700322>
- Yang, X. Y., He, K., Pan, C. S., Li, Q., Liu, Y. Y., Yan, L., ... Han, J. Y. (2015). 3,4-Dihydroxy-phenyl lactic acid restores NADH dehydrogenase 1  $\alpha$  subunit 10 to ameliorate cardiac reperfusion injury. *Scientific Reports*, 5, 10739. <https://doi.org/10.1038/srep10739>
- Yin, Q., Lu, H. Y., Bai, Y. J., Tian, A. J., Yang, Q. X., Wu, J. M., ... Li, Z. (2015). A metabolite of Danshen formulae attenuates cardiac fibrosis induced by isoprenaline, via a NOX2/ROS/p38 pathway. *British Journal of Pharmacology*, 172(23), 5573–5585. <https://doi.org/10.1111/bph.13133>
- Zhang, L., Lv, L., Chan, W. M., Huang, Y., Wai, M. S., & Yew, D. T. (2012). Effects of DL-3-n-butylphthalide on vascular dementia and angiogenesis. *Neurochemical Research*, 37, 911–919. <https://doi.org/10.1007/s11064-011-0663-3>
- Zhang, Q., & Kelley, E. (2014). The WHO traditional medicine strategy 2014–2023: A perspective. *Science*, 346(6216Suppl), S5–S6.
- Zhao, S., & Li, S. (2010). Network-based relating pharmacological and genomic spaces for drug target identification. *PLoS ONE*, 5(7), e11764.
- Zhao, X., Zheng, X., Fan, T., Li, Z., Zhang, Y., & Zheng, J. (2015). A novel drug discovery strategy inspired by traditional medicine philosophies. *Science*, 347(6219Suppl), S38–S40.
- Zheng, X. H., Jia, P., & Bai, Y. J. (2015). Research strategy for combination of traditional Chinese medicine molecular chemistry based on the traditional theory of “Jun-Chen-Zuo-Shi”. *Journal of Northwest University. Natural Science Edition*, 45, 405–412.
- Zheng, X. H., Zhao, X., Fang, M. F., Wang, S. X., Wei, Y. M., & Zheng, J. B. (2007). Pharmacokinetic effects of Shi herb-borneol on Jun herb-*Salvia miltiorrhiza*. *Journal of Xi'an Jiaotong University (Medical Sciences)*, 28(2), 170–173.
- Zheng, X. H., Zhao, X. F., Zhao, X., Wang, S. X., Wei, Y. M., & Zheng, J. B. (2007). Determination of the main bioactive metabolites of Radix *Salvia miltiorrhizae* in compound Danshen dripping pills and the tissue distribution of Danshensu in rabbit by SPE-HPLC-MSn. *Journal of Separation Science*, 30(6), 851–857.
- Zhu, X. Y., Daghini, E., Chade, A. R., Lavi, R., Napoli, C., Lerman, A., & Lerman, L. O. (2008). Disparate effects of simvastatin on angiogenesis during hypoxia and inflammation. *Life Sciences*, 83(23–24), 801–809. <https://doi.org/10.1016/j.lfs.2008.09.029>
- Zudaire, E., & Cuttitta, F. (2012). *The textbook of angiogenesis and lymphangiogenesis: Methods and applications*. Netherlands: Springer. <https://doi.org/10.1007/978-94-007-4581-0>

## SUPPORTING INFORMATION

Additional supporting information may be found online in the Supporting Information section at the end of the article.

**How to cite this article:** Liao S, Han L, Zheng X, et al. Tanshinol borneol ester, a novel synthetic small molecule angiogenesis stimulator inspired by botanical formulations for angina pectoris. *Br J Pharmacol*. 2019;176:3143–3160. <https://doi.org/10.1111/bph.14714>